

- 1 Phytoplankton biodiversity and cellular acclimation to vertical nutrient flux ratio
- 2 control particulate stoichiometry in the North Atlantic, according to field observations
- 3 of cellular elemental stoichiometry across taxonomic groups and ocean basins.

1 **Peer review information:** Communications Earth & Environment thanks the anonymous reviewers for
2 their contribution to the peer review of this work. Primary Handling Editors: Clare Davis.

3 **Varying influence of phytoplankton biodiversity and stoichiometric plasticity on bulk
4 particulate stoichiometry across ocean basins**

5
6
7 Michael W. Lomas^{1*}, Steven E. Baer², Celine Mouginot³, Kristina X. Terpis⁴, Debra A. Lomas¹,
8 Mark A. Altabet⁵, Adam C. Martiny^{3,6}

9
10 ¹ Bigelow Laboratory for Ocean Sciences, East Boothbay, ME 04544, USA
11 ² Corning School of Ocean Studies, Maine Maritime Academy, Castine, ME 04420, USA

12 ³ Department of Earth System Science, University of California at Irvine, Irvine, CA 92697,
13 USA

14 ⁴ Department of Biological Sciences, University of Rhode Island, Kingston, RI 02881, USA

15 ⁵ School of Marine Science and Technology, University of Massachusetts Dartmouth, New
16 Bedford, MA 02067, USA

17 ⁶ Department of Ecology and Evolution, University of California at Irvine, Irvine, CA 92697,
18 USA

19
20
21 * **Corresponding author:** Michael W. Lomas, mlomas@bigelow.org, 011-207-315-2567 ext.
22 311, ORCID Number: 0000-0003-1209-3753

23
24 **Key Words:** phytoplankton, elemental stoichiometry, nutrient ratios, biodiversity

25
26 **Proposed Journal:** Communications Earth and Environment

28 **Abstract**

29 Concentrations and elemental ratios of suspended particulate organic matter influence many
30 biogeochemical processes in the ocean, including patterns of phytoplankton nutrient limitation
31 and links between carbon, nitrogen and phosphorus cycles. Here we present direct measurements
32 of cellular nutrient content and stoichiometric ratios for discrete phytoplankton populations
33 spanning broad environmental conditions across several ocean basins. Median cellular carbon-
34 to-phosphorus and nitrogen-to-phosphorus ratios were positively correlated with vertical nitrate-
35 to-phosphate flux for all phytoplankton groups and were consistently higher for cyanobacteria
36 than eukaryotes. Light and temperature were inconsistent predictors of stoichiometric ratios.
37 Across nutrient-rich and phosphorus-stressed biomes in the North Atlantic, but not in the
38 nitrogen-stressed tropical North Pacific, we find that a combination of taxonomic composition
39 and environmental acclimation best predict bulk particulate organic matter composition. Our
40 findings demonstrate the central role of plankton biodiversity and plasticity in controlling
41 linkages between ocean nutrient and carbon cycles in some regions.

42

43 **Introduction**

44 Marine phytoplankton elemental stoichiometry has received a significant amount of new
45 attention over the past decade from both observational and theoretical points of view, given the
46 central role of stoichiometric ratios in understanding global patterns in primary production,
47 carbon export and interconnectivity between trophic levels^{1,2}. Eight decades ago Alfred C.
48 Redfield observed that the mean ratio of sestonic particulate organic carbon (C) to nitrogen (N)
49 to phosphorus (P) was similar across ocean regions at 106:16:1, albeit with wide ranges in
50 values, and was similar to the dissolved inorganic nutrient ratios in the deep ocean. Redfield
51 hypothesized that this global mean state was due to the remineralization of sinking particulate
52 material derived from the stoichiometric preferences of phytoplankton³ but did not rule out
53 regional patterns in phytoplankton community selection and/or nitrogen cycle feedbacks⁴. As
54 data has accumulated, consistent spatial patterns of deviation from the Redfield Ratio have
55 emerged, although the underlying mechanisms continue to be debated.

56 Spatial variability in the average taxonomic composition of natural phytoplankton
57 populations has been hypothesized as an important driver of observed patterns in bulk particulate
58 stoichiometry^{5,6}. For example, diatoms^{7,8}, which thrive in nutrient-rich environments, commonly
59 display N:P ratios lower than the Redfield Ratio, while in contrast, cyanobacteria, which thrive
60 in nutrient-poor environments, commonly display N:P ratios greater than the Redfield Ratio in
61 culture⁹. C:N ratios, in contrast, range much more narrowly among taxa. While broad
62 taxonomically-linked stoichiometric ratios are observed⁵, they are not constant, as within a given
63 phytoplankton taxa phenotypic acclimation to nutrient conditions does occur^{10,11}. Similarly, in
64 the subtropical N. Atlantic it has been shown that specific phytoplankton taxa from natural
65 populations have different stoichiometric ratios as a function of depth at the same station⁵.
66 Sharoni and Halevy⁶, based on a meta-analysis of field data, concluded that phytoplankton
67 community composition, using ‘optimum-growth’ mean cellular stoichiometries associated to

68 each taxonomic group, was a better predictor of bulk particulate N:P ratios than a nutrient
69 concentration acclimation model. Reaching a different conclusion, Galbraith and Martiny¹²
70 observed a robust relationship between ambient phosphate concentrations and bulk particulate
71 N:P ratios, which was mechanistically linked to plasticity in the ability of certain phytoplankton
72 to modulate phosphorus content. The results of these two studies are not mutually exclusive, due
73 to the covariance of elevated nutrient concentrations and phytoplankton communities dominated
74 by diatoms¹³.

75 In assessing phytoplankton elemental stoichiometry, measurement of bulk POM ratios
76 leads to biases of varying degrees through the inclusion of heterotrophic and detrital particles¹⁴⁻
77¹⁶. Inclusion of detrital particles can lead to elevated POM ratios, in nutrient depleted regions¹⁷,
78 independent of the living phytoplankton community. Latitudinal patterns of elevated POM ratios
79 in the tropics and lower ratios in polar waters could thus result from the additive patterns of
80 decreasing relative contribution of detrital particles and increasing prevalence of diatoms from
81 the equator to the poles. While studies have concluded that phytoplankton biodiversity is a more
82 important driver of POM composition^{5-8,18}, these studies, except for those of Martiny et al.⁵ and
83 Baer et al.¹⁸, have only correlated patterns in biodiversity with bulk POM composition. Further,
84 disentangling phytoplankton community from phenotypic plasticity within a taxonomic group is
85 an extant challenge, and this study presents direct observational data focused on this challenge.
86 This study addresses the following questions. What is the variability in element contents and
87 stoichiometric ratios for specific phytoplankton populations across ocean regions? Does
88 environmental forcing modulate the observed stoichiometric ratios within a taxonomic group?
89 Do shifts in biodiversity contribute to variation in bulk C:N:P of marine communities?

90

91 **Results and Discussion**

92 **Cellular Macronutrient Contents.** Only in the North Atlantic have studies directly measured
93 stoichiometric ratios in phytoplankton taxa physically separated from natural populations.
94 Results highlighted the first order role of phytoplankton biodiversity for determining variations
95 in elemental ratios^{5,18}. In contrast, in the eastern Indian Ocean, with muted variability in
96 phytoplankton biodiversity, relative to the North Atlantic, studies of bulk POM stoichiometry
97 identified an important role for nutrient supply, using nutricline depth as a proxy¹⁹. Coupled trait-
98 based/remote-sensing input models applied to the global ocean reach equally diverse conclusions
99 of the importance of biodiversity⁶ versus nutrient inputs when applied to the global ocean¹⁵.
100 Here, we present a dataset collected from several major ocean basins and a range of
101 environments (**Figure 1**) where we have used fluorescence-activated cell sorting to isolate
102 populations of important picocyanobacteria, *Prochlorococcus* and *Synechococcus*, and an
103 operationally defined picoeukaryotic phytoplankton for subsequent analysis of their elemental
104 macronutrient content and calculated stoichiometric ratios. The dataset comprises results from
105 samples sorted both live (immediately at sea) and those fixed and sorted in the shore-side
106 laboratory, as the difference between them in paired samples was found to be acceptably small
107 (**Supplementary Figure 1**). For a given element, cellular contents generally spanned a similar
108 range between different biogeographic regions (**Figure 2** and **Supplementary Table 2**), showing

109 no discernable regional control on cell nutrient content. Elemental concentrations of C from
110 field populations generally agreed well with the range of values previously summarized²⁰; 2-28
111 fmol C cell⁻¹, 4 – 77 fmol C cell⁻¹, and 4 – 795 fmol C cell⁻¹ for *Prochlorococcus*, *Synechococcus*
112 and picoeukaryotes, respectively. Although in some instances (e.g., ETNP) measured values for
113 *Prochlorococcus* and *Synechococcus* exceeded the published range, but by no more than a factor
114 of two. Published data for cellular N and P content are more scarce, however, values determined
115 in this study agree within a factor of two of published data from culture studies (**Figure 2**).

116

117 **Stoichiometric Ratios.** We explored elemental stoichiometric ratios between different
118 taxonomic populations to determine if previously observed taxonomic differences in the North
119 Atlantic^{18,21} are observed in other regions. *Prochlorococcus* and *Synechococcus* populations,
120 consistently were found to have mean elemental C:N (11±4; 9±2, respectively), C:P (228±77;
121 188±68, respectively) and N:P (22±9; 21±7, respectively) ratios that were 0.5 to 2-fold higher
122 than the canonical Redfield Ratio^{3,4}. In contrast, the C:N (7±2), C:P (103±15) and N:P (15±4)
123 ratios of co-occurring eukaryotes were both less variable and much closer to the Redfield Ratio
124 (**Figure 3** and **Supplementary Table 3**; Taxa x Region ANOVA, all pairwise comparisons P-
125 value < 0.01). There were exceptions, such as the nutrient-rich Peru upwelling (Peru UW) where
126 *Synechococcus* C:P ratios were similar to the C:P ratio of co-occurring eukaryotes, and the
127 subpolar N. Atlantic (NASP), where *Synechococcus* had a median C:P ratio that was twice that
128 of co-occurring eukaryotes, but was still low compared to other regions in the dataset. In these
129 two nutrient-rich systems, *Prochlorococcus* was not present in sufficient numbers to sort for a
130 meaningful elemental analysis, so we cannot assess if this is a general cyanobacterial response to
131 nutrient-rich conditions. The Pacific equatorial upwelling, which is intermediate in near-surface
132 nutrient concentrations and where *Prochlorococcus* populations were sorted, did not elicit a
133 reduced C:P ratio in either cyanobacterial population. Significant differences in stoichiometric
134 ratios between *Prochlorococcus* and *Synechococcus* were only observed in the NASG.
135 Comparisons within a taxonomic group between different regions showed no significant
136 differences, although median values often varied by 25-50% between regions.

137 Why are elemental stoichiometric ratios of cyanobacteria, in nutrient-deplete ocean
138 regions, consistently higher than the canonical Redfield Ratio and that of co-occurring
139 eukaryotes? To explore if these differences are due to elevated C content or reduced N and P
140 contents, we compare our data to published elemental quota data (**Supplementary Figure 2**).
141 Given the unknown, but quite likely variable, physiological state of the field samples in this
142 study, published data were taken from both culture and natural population data, and which
143 included both nutrient-replete and nutrient-deplete growth conditions. The literature values are
144 presented with their complete range to better reflect this wide range of environmental variables
145 and growth conditions. *Prochlorococcus* (80 ± 27 fmol μm^{-3}) and *Synechococcus* (46 ± 30 fmol
146 μm^{-3}) were found to have mean cell C quotas outside the range of published values, 15 – 40 fmol
147 μm^{-3} (22-24). The sorted eukaryotic populations, unlike the picocyanobacteria populations, are
148 a diverse mix of taxa grouped by similarity in size. Small eukaryotes, deemed similar in size to
149 those sorted in this study, have a C quota range of 9-18 fmol μm^{-3} (25,26), a range which is higher

150 than the mean cell quota observed in this dataset, $5 \pm 2 \text{ fmol } \mu\text{m}^{-3}$. Similar patterns are seen for
151 N and P quotas. Mean N quotas for *Prochlorococcus* ($8 \pm 3 \text{ fmol } \mu\text{m}^{-3}$) and *Synechococcus* ($5 \pm$
152 $3 \text{ fmol } \mu\text{m}^{-3}$) are greater than the range found in the literature, 1.4-4.0 fmol μm^{-3} (9,24), while the
153 mean N quota of eukaryotes ($0.6 \pm 0.4 \text{ fmol } \mu\text{m}^{-3}$) was within the estimated published range (0.3
154 - 2 fmol μm^{-3} , 9,26). Mean P quotas for *Prochlorococcus* ($0.2 \pm 0.1 \text{ fmol } \mu\text{m}^{-3}$) and
155 *Synechococcus* ($0.1 \pm 0.1 \text{ fmol } \mu\text{m}^{-3}$) are more similar to the range found in the literature, 0.03-
156 $0.12 \text{ fmol } \mu\text{m}^{-3}$ (9,24), while the mean P quota of eukaryotes ($0.04 \pm 0.03 \text{ fmol } \mu\text{m}^{-3}$) was within
157 the estimated published range ($0.02 - 0.25 \text{ fmol } \mu\text{m}^{-3}$, 9,26-28). This analysis suggests a
158 fundamental difference between natural populations of cyanobacteria and eukaryotes of similar
159 size, with cyanobacteria from this study consistently showing greater cell C quotas than
160 previously published data, while eukaryotes consistently show lower cell C quotas. Although the
161 physiological mechanisms cannot be confirmed with the data in hand, our data are consistent
162 with prior research that found significantly greater biomass specific C fixation rates in
163 cyanobacteria than co-occurring eukaryotes²⁹, which may lead to the observed increases in C
164 quotas.

165

166 **Environmental Correlates.** We explore environmental controls to explain the variability in cell
167 contents and stoichiometric ratios (**Table 1** and **Supplementary Figures 3-7**). First, we use
168 depth as a proxy for the light environment to which the cells were exposed. Across the entire
169 dataset, C content in *Prochlorococcus* increased significantly (Model 1 regression, $P < 0.05$)
170 with depth, while P content in *Prochlorococcus* exhibited a marginally significant increase with
171 depth. A similar pattern for C has been reported previously in data from the subtropical North
172 Atlantic²⁰ and cultures³⁰. The only other significant relationship observed with depth was for
173 *Synechococcus* N content. This is likely due to photoacclimation and increases in cellular
174 pigments containing N^{31,32}. Chlorophyll has 4 N atoms in its structure and thus increases in
175 chlorophyll pigment would increase cellular nitrogen content, although it would increase C
176 content to a greater degree (chlorophyll C:N ratio 13.5:1). It is more likely that an increase with
177 depth in N-rich phycobilisomes³³ led to the increase in *Synechococcus* cellular N quota without
178 an increase in C (**Table 1** and **Supplementary Figure 3 and 6**). This explanation also is
179 consistent with the lack of relationship between N quota and depth for *Prochlorococcus*, as this
180 genera does not use phycobilisomes, but rather a much more N efficient light harvesting
181 system^{34,35}.

182 Temperature is known to regulate a wide range of physiological and cellular
183 processes^{36,37}. Across the entire dataset, *Prochlorococcus* showed a significant negative
184 relationship between cellular C content and temperature, while *Synechococcus* showed a
185 significant negative relationship between cellular P content and temperature (**Table 1** and
186 **Supplementary Figure 4**). The observations for *Synechococcus* and P content are consistent
187 with lab studies^{38,39}, although the observations for *Prochlorococcus* are not. In general,
188 however, these trends in cyanobacteria populations are consistent with the notion that higher
189 temperatures are associated with ocean gyres, which are more likely to be nutrient deplete
190 leading to a range of physiological adjustments including higher relative rates of release for

191 newly fixed C (⁴⁰) and reductions in cellular P-containing metabolites⁴¹. In contrast, for the
192 Eukaryotes, there is a marginally significant (**Table 1**) positive relationship between both
193 cellular C and P and temperature. Further, the trend in the data presents itself as an “envelope”
194 setting a maximum upper limit rather a predictive relationship between variables
195 (**Supplementary Figure 4**). While physiological versus taxonomic differences cannot be
196 resolved for this ‘population’ as it contains an unknown diversity of eukaryotes of similar size,
197 the observation of increasing cell contents is consistent with phytoplankton temperature
198 dependent growth response envelopes⁴² and the observed differential responses to increasing
199 temperature between cultured strains³⁶.

200 Nearly half of the cellular stoichiometric ratios showed a significant, or marginally
201 significant, relationship with temperature (**Table 1** and **Supplementary Figure 7**). C:P ratios,
202 but not N:P ratios, for *Synechococcus* and eukaryotes were positively related with temperature;
203 an observation consistent with recent research^{43,44}. In this study, for *Synechococcus* the increase
204 in C:P ratio is the result of reduced P contents with temperature, consistent with the temperature-
205 dependent physiology hypothesis⁴⁵. However, for the eukaryotes the response was more
206 complicated, due to the observation that both cellular C and P increased with temperature
207 (**Supplementary Figure 4**), although the greater temperature sensitivity of C, relative to P, led
208 to the significant increase in C:P. The relationships between C:N:P and temperature are more
209 complex and species-specific than presented by Yvon-Durocher⁴⁴.

210 Absolute nutrient concentrations, and nutrient ratios are well known to regulate cellular
211 particulate stoichiometric ratios in a wide range of species⁴⁶. Here, we examined nutrient ratios
212 in two formats; the ratio of ambient residual nutrient stocks at the depth from which samples
213 were collected, and the ratio of vertical nutrient fluxes across the nutricline, which in most cases
214 was at the base of the euphotic zone (see Baer et al.^{18,47} for more information on this approach).
215 The nutrient flux ratio is more impactful to phytoplankton in the deepest samples as this
216 represents the ratio supplied by vertical mixing and upwelling⁴⁸. No cell contents or
217 stoichiometric ratios were significantly correlated with measured ambient residual
218 nitrate:phosphate nutrient ratios. While this result is in contrast to recent publications², it is not
219 unexpected given that surface concentration ratios are not expected to be representative of
220 phytoplankton uptake ratios and further are skewed by analytical uncertainty at low ambient
221 nutrient concentrations which can impact ratio calculations.. In contrast, *Prochlorococcus* and
222 *Synechococcus* both showed cell contents that were negatively correlated with increasing ratios
223 of vertical nitrate:phosphate fluxes (**Supplementary Figure 5**). This relationship appeared more
224 as a ‘threshold’, where above nitrate:phosphate flux ratios of ~24:1 cell contents of C and P
225 attained a minimum and remained at this level while at flux ratio values less than ~24:1, cell
226 contents spanned the entire observed range. This type of inverse rectilinear response is very
227 similar to the response seen in critical nutrient ratio experiments^{11,49} that demonstrate the
228 nitrate:phosphate availability ratio where cells transition from N to P limitation. While
229 eukaryote cell contents were not significantly correlated with nitrate:phosphate flux ratios, and
230 cell contents did not demonstrate the rectilinear response seen in the cyanobacteria lineages,
231 there was an upper limit to observed cell content values, which did decrease with increasing
232 nitrate:phosphate flux ratios.

233 Of the environmental variables examined, it was the vertical nitrate:phosphate flux ratios
234 that most consistently (8 out of 9 relationships were significant or marginally so) explained
235 variance in elemental stoichiometric ratios. As anticipated, vertical nitrate:phosphate flux ratios
236 were positively correlated with C:P and N:P ratios in all taxonomic groups, although the
237 magnitude of the response varied (**Figure 4** and **Table 1**). The cyanobacterial populations
238 displayed a greater increase in C:P and N:P ratios than the eukaryotes, an observation consistent
239 with previous work by this group of researchers⁵. The increases in C:P and N:P ratios are driven
240 primarily by decreases in cellular P contents (**Supplementary Figure 5**), as expected, in
241 response to increasing P-stress. The damped response of C:P and N:P ratios in eukaryotes could
242 arise from nutrient co-limitations⁵⁰ that limit their plasticity with regard to P. For example, it has
243 been shown that eukaryotes, in response to extreme P-stress replace P-containing lipids with N-
244 containing lipids⁴¹. In the nutrient deplete regions, where most of these samples were collected,
245 N concentrations are also exceedingly low and thus may limit the ability of eukaryotes to
246 modulate their P content. In contrast, the cyanobacteria genera readily swap P-containing lipids
247 for sulfur containing lipids. Perhaps a more likely explanation is that eukaryotes are
248 supplementing their autotrophic nutrition with mixotrophy⁵¹. Pigmented eukaryotes of the size
249 that were sorted in this study have been shown to dominate bacterivory in the ocean and can
250 obtain up to 25% of the nutrient demand from this mixotrophic nutritional mode⁵².

251 C:N ratios in *Prochlorococcus*, but not *Synechococcus* were negatively related to vertical
252 nitrate:phosphate flux ratios, but this is largely driven by high cellular C:N values when vertical
253 nitrate:phosphate flux ratios decreased below the Redfield Ratio of 16:1. This suggests that
254 below a flux ratio of 16:1, conditions of increasing relative N-stress, *Prochlorococcus* continues
255 to accumulate cellular C via photosynthesis²⁹ although there are questions on whether that newly
256 fixed C is retained^{40,53}. In contrast, the eukaryotic C:N ratios were positively correlated with
257 nitrate:phosphate flux ratios, driven by a greater relative reduction in N content than C content in
258 response to increasing vertical nitrate:phosphate flux ratios. The observation that within a
259 taxonomic group variance in stoichiometric ratios can be explained by the relative input of
260 potentially limiting macronutrients suggests that the optimal allocation phytoplankton model
261 proposed by Sharoni and Halevy may have more than one ‘solution’ or is not always the best
262 model to explain bulk particulate organic matter stoichiometric ratios⁶.

263

264 **Predicting Particulate Organic Matter Ratios.** Due to the analytical challenges associated
265 with generating these data, directly assessing the relationships between phytoplankton
266 stoichiometry and bulk POM at broader scales is difficult. To assess if taxonomic variability in
267 stoichiometric ratios was an important control on bulk POM ratios⁶⁻⁸, we evaluated two models
268 for prediction of bulk POM stoichiometric ratios. First, was the ‘optimal-growth’ phytoplankton
269 model that only takes into consideration the relative abundance of taxonomic groups and a mean
270 stoichiometric ratio for each group⁶. In this model, the relative C biomass abundance of
271 taxonomic groups was scaled by a constant mean group-specific stoichiometric ratio compiled
272 from the published literature (**Supplementary Table 4**). The predicted POM stoichiometry is
273 the weighted mean of the relative abundance of phytoplankton taxa multiplied by these ratios.

274 Because the model assumes that the resident phytoplankton are growing at an invariant
275 ‘optimum’ stoichiometric ratio, then any relationships between observed bulk POM ratios and
276 this model output results from changes in phytoplankton community composition. Second, we
277 assessed an ‘acclimation’ model that considers the relative abundance of taxonomic groups,
278 identical to the optimum-growth model, but calculates a sample-specific stoichiometric ratio
279 rather than using the literature-based optimum value. A multiple linear regression model was
280 used to calculate the group-specific stoichiometric ratios based upon the temperature, depth and
281 vertical nitrate:phosphate flux ratios (**Supplementary Table 5**), at each station/depth, which was
282 then scaled to the relative C biomass of each group in this model. We used both models to
283 predict bulk POM stoichiometric ratios, which this research team directly measured along
284 transects from 19°N to 55°N in the western N. Atlantic Ocean and from 19°N to 3°S in the
285 central Tropical/Equatorial Pacific (**Figure 5** and **Supplementary Figure 8-9**).

286 Both models provided a reasonable representation of the bulk particulate stoichiometric
287 ratios over portions of both transects (**Figure 5** and **Supplementary Figure 8-9**). This suggests
288 that to a first order phytoplankton community composition is an important driver of bulk POM
289 stoichiometry ratios, otherwise model output and observations would not agree as often as was
290 seen. However, our dataset does not have a great enough ‘dynamic range’ in the phytoplankton
291 community composition, most samples were from oligotrophic regions and we did not quantify
292 large phytoplankton in the nutrient rich regions, to find a significant predictive correlation
293 between phytoplankton communities and bulk POM ratios.

294 C:N ratios varied little along either transect with no significant differences between
295 observations and model outputs (**Supplementary Figure 8**). This result for C:N ratios is perhaps
296 expected as prior studies have shown similarly narrow ranges of bulk POM C:N ratios²¹.
297 Furthermore, different picoplankton populations from the western North Atlantic, flow
298 cytometrically sorted as in this study, are only marginally different from each other in terms of
299 the C:N ratios²¹. Bulk POM N:P ratios showed expected trends, with bulk POM N:P ratios along
300 the N. Atlantic transect increasing from ~10:1 in the north to ~20:1 in the south, while along the
301 tropical Pacific transect values remained roughly constant at ~20:1 (**Supplementary Figure 9**).
302 Significant differences between model outputs and bulk POM N:P ratios were few, and only
303 occurred at the transition from the subpolar gyre to the subtropical gyre (~40°N) along the N.
304 Atlantic transect. While differences were not significant for most stations, mean N:P ratios from
305 the optimal-growth model were consistently greater than N:P values from the acclimation model
306 as the fixed stoichiometric N:P ratios in the optimum-growth model were not fully compensated
307 by the shift from a population dominated by cyanobacteria to one dominated by eukaryotes. This
308 result supports the hypothesis that phytoplankton community structure and acclimation to local
309 conditions interact to modulate stoichiometric ratios in these populations. Changes in
310 stoichiometric C:P ratios more clearly highlighted the potential interplay between phytoplankton
311 community composition and acclimation to the local environment. Along the N. Atlantic
312 transect, bulk POM stoichiometric ratios significantly increased (station by station comparison,
313 Student’s t-test, $P < 0.05$) once south of ~30°N, an observation previously noted in this region⁵
314 and consistent with the hypothesis that this region is P-stressed⁵⁴⁻⁵⁶. The stoichiometric ratios
315 from the optimal-growth model increased only slightly, due to the increase in relative biomass of

316 *Prochlorococcus*, and were significantly lower than the bulk POM stoichiometric ratios. In
317 contrast, the stoichiometric ratios from the acclimation model tracked bulk POM in this region
318 and were not significantly different, supporting contention of nutrient control of stoichiometric
319 ratios². Furthermore, this increase in bulk POM and acclimation model stoichiometric ratios is
320 consistent the increase in the vertical nitrate:phosphate flux ratio along this transect¹⁸. The
321 transect in the tropical Pacific however, did not show any significant differences between either
322 model and the observed bulk POM stoichiometric ratios, despite similarly low nutrient
323 concentrations over much of the transect. A possible explanation for this is the suggestion that
324 the Pacific in this region could be N-stressed⁵⁷, rather than P-stressed. At least for
325 *Synechococcus*, N-stress has been shown to have no meaningful impact on any of the
326 stoichiometric ratios, unlike P-stress which leads to significant changes in the N:P and C:P
327 ratios⁵⁸. If the nutrient-stress response of stoichiometric ratios seen in *Synechococcus* is mirrored
328 in *Prochlorococcus*, the dominance of *Prochlorococcus* in the autotrophic community could
329 definitely explain the limited variability in bulk stoichiometric ratios and the lack of difference
330 between the optimal-growth and acclimation models.

331 These models show that controls on bulk POM stoichiometry are more complicated than
332 recently concluded⁶. Both phytoplankton biodiversity and acclimation to the local environment
333 are important controlling factors of bulk POM stoichiometry and these controls differ between
334 ocean regions. Sharoni and Halevy recently concluded that phytoplankton are well-adapted to
335 their ambient nutrient environment in all ocean regions modeled, however, our data show that it
336 is the ratio of nitrate:phosphate inputs that drives cellular acclimation responses, a conclusion
337 also reached in chemostat culture studies¹⁰. We conclude that biogeochemical models should
338 include both phytoplankton biodiversity and cellular acclimation to vertical nutrient flux ratio
339 controls in predictions of particulate stoichiometry and ocean biogeochemistry.

340

341 **Concluding Remarks**

342 Our observations of cellular macronutrient, C, N and P, content in populations of marine
343 cyanobacteria and small eukaryotes from a wide range of ocean regions are generally consistent
344 with data from cultured strains, but present a significant advance as they are direct measures of
345 field populations. The resulting stoichiometric ratios confirmed prior observations of
346 cyanobacteria having consistently and significantly higher ratios than co-occurring eukaryotes,
347 with one notable exception. *Synechococcus* populations in the nutrient-enriched Peru upwelling
348 region displayed C:P and N:P ratios that were similar to that of eukaryotes. This observation
349 supports our conclusion that while baseline stoichiometric ratios are taxonomically linked;
350 cellular ratios are not ‘fixed’ but rather are modulated in response to the local environment, in
351 particular nutrient inputs. Whether this modulation arises purely from physiological plasticity or
352 from changes in a dominant genotype, particularly in cyanobacteria⁵⁹, remains to be completely
353 resolved.

354 Ambient light levels (using collection depth as a proxy) and temperature were not found to
355 be consistent environmental drivers and only a subset of element/taxa combinations were

356 significantly related to these environmental variables. In stark contrast, the ratio of
357 nitrate:phosphate mixing into the euphotic zone across the nutricline correlated with nearly all
358 element/taxa cell contents and stoichiometric ratios. This highlights that despite recent
359 assertions, evidence from direct observations, shows that physiological acclimation to local
360 nutrient supply is important to understand variance in observed cellular macronutrient contents
361 and stoichiometric ratios, and that the degree of acclimation may differ between prokaryotic and
362 eukaryotic taxa. Further, predictions of particulate C:P ratios compared more favorably when
363 this environmental acclimation was considered.

364

365 Methods

366 *Phytoplankton sample collection and preparation.* Samples were collected from cruises in
367 several major ocean basins (**Supplementary Table 1**). Samples for taxon-specific elemental
368 content were collected using 12L Niskin bottles, along with electronic CTD sensor data
369 (temperature, salinity, *in vivo* chlorophyll fluorescence, dissolved oxygen), usually from two
370 depths at each station; one within the upper mixed layer (10-20m) and one near the deep
371 chlorophyll maximum. Due to timing of the cruises, samples were collected from a seasonal
372 window limited to summer and early fall. Samples were prepared for sorting by concentrating
373 cells from the ambient sample under darkened conditions using a Memteq High Volume Cell
374 Trap (0.2 μ m pore size)⁶⁰, and then flushed from the Cell Trap using 0.2 μ m filtered seawater
375 and a luer lock syringe; roughly 3-4L of ambient seawater was concentrated down to ~5mls.
376 Samples were either gravity filtered through the Cell Trap directly from the Niskin bottle or
377 pushed through the cell trap using a peristaltic pump at <50ml min⁻¹. Samples were then kept
378 cool at 4°C if they were going to be sorted live and immediately after collection or fixed with
379 freshly filtered paraformaldehyde (0.5% v/v final concentration) if they were going to be stored
380 for later sorting. Samples were allowed to fix at 4°C for 1-2h and then flash frozen in liquid
381 nitrogen and then moved to -80°C for longer term storage.

382

383 *Cell sorting and elemental analysis.* The cell counting and sorting protocols used follow that of
384 Baer et al.¹⁸ as summarized here. Cell counts and sorts were performed on either a Becton
385 Dickinson Influx or FACSJazz flow cytometer, each utilizing a 200 mW 488 nm laser, with
386 detectors for forward scatter, side scatter, 692 nm, and 530 nm, and operated with 8g NaCL kg⁻¹
387 solution for sheath fluid, which was filtered inline using a 0.22 μ m Millipore Sterivex™ filter.
388 Instrument alignment was performed with 3.0 μ m 6-peak rainbow beads, while roughly hourly
389 checks on forward scatter response were performed with 0.53 μ m Nile Red beads (Spherotech).
390 *Prochlorococcus* populations were discriminated based on forward scatter and red fluorescence,
391 and a gate in orange (530 nm) discriminated for *Synechococcus*. Eukaryotes were all larger
392 autofluorescing cells that did not fit the cyanobacterial gating scheme. For sorting, sort control
393 software was set to “1.0 drop pure” sort mode. In excess of 17 million, 8 million, and 500,000
394 cells for *Prochlorococcus*, *Synechococcus*, and eukaryotes were sorted for chemical analysis,
395 respectively. Not all phytoplankton groups were sufficiently abundant at each station/depth for
396 practical sorting and subsequent analysis. Post-sort purity tests were run with subsamples of each
397 sorted population; sort purity always exceeded 94%. Sorted populations were collected in
398 polystyrene Falcon tubes (BD Biosciences Inc.) and subsequently filtered on pre-combusted

399 (450°C for 4 hours) GF-75 filters (Ahlstrom; nominal pore size = 0.3 μm). To ensure complete
400 capture of all of the cells, the Falcon tubes were rinsed multiple times with 0.2 μm filtered sheath
401 fluid. Filter and sheath fluid blanks were produced each day samples were sorted for subsequent
402 subtraction from the mass of each unknown sample. Following filtration, filters were placed in
403 acid-washed cryovials and frozen (-20°C) until analysis as described below. Average cellular
404 elemental content was determined by dividing the elemental content of the sample by the number
405 of sorted cells as determined in a direct post-sort count analysis of the sorted sample. Data are
406 publicly accessible⁶¹.

407 *Dissolved Nutrients and fluxes.* Nutrient samples were collected after filtration through 0.8 μm
408 polycarbonate filters. Inorganic nutrient concentrations were analyzed using standard protocols
409 and calibrations on an air-segmented autoanalyzer⁶²⁻⁶⁴; NO_3^- detection limit = 30 nmol N kg^{-1} ,
410 and PO_4^{3-} detection limit = 50 nmol kg^{-1} . On all cruises, except for NH1410, SO243, RR1604,
411 SPOTS and Newport Pier, soluble reactive P (SRP) concentrations were also measured via the
412 magnesium-induced co-precipitation method^{65,66} with modifications as per Lomas et al.⁵⁵;
413 detection limit = 1 nmol P kg^{-1} . P sample concentrations were calculated against a potassium
414 monobasic phosphate standard prepared in P-free seawater⁵⁵, and a certified phosphate standard
415 (Ocean Scientific International Ltd. Phosphate Nutrient Standard Solution) was used for quality
416 control with each analytical run.

417 Diapycnal nitrate:phosphate flux ratios were calculated directly from the slope of nutrient
418 concentration profiles under the assumption that the vertical diffusivity coefficients would apply
419 equally to both nutrients, and thus a value for diffusivity was not needed in the calculation. The
420 slope of the nutrient profile was calculated across the nutricline, defined as the depth where
421 nutrient concentrations exceeded the analytical limit of quantitation for each nutrient, which
422 varied from region to region depending upon local conditions.

423 *Particulate nutrients.* Particulate organic P (POP) was analyzed using the ash-hydrolysis
424 method⁵⁵, with oxidation efficiency and standard recovery tested with each sample run using an
425 ATP standard solution and a certified phosphate standard (OSIL Phosphate Nutrient Standard
426 Solution). Method precision is 1-2% at 5 nmol kg^{-1} . Samples for POC and PON were acid
427 fumed in a desiccator over concentrated HCl prior to analysis. After acid fuming, POC and PON
428 were determined on a Costech 4010 elemental analyzer or a Control Equipment 440 elemental
429 analyzer, depending on the samples. L-glutamic acid (USGS40) was used for standard curve
430 generation and as a check standard (tolerance of <0.1 μg) approximately every ten samples and
431 at the end of every instrument run. Empty tin capsules (Costech Analytical Technologies) were
432 cleaned with acetone and dried and run as instrument blanks.

433 *Elemental Stoichiometry Models.* The elemental cell quota data determined in this study were
434 used in mathematical models to estimate calculated phytoplankton community stoichiometric
435 ratios in comparison to concurrent measurements of bulk particulate organic matter ratios
436 (**Supplementary Data 1**). Full details of model calculations are provided in the Supplemental
437 Information text. In brief, two models were used, one was an optimal-growth model using
438 cellular stoichiometric data from culture experiments in the published literature (**Supplementary**
439 **Table 4**) where growth rates were not limited. The other model was an acclimation model where
440 elemental cell quota data collected in this study were related to ambient environmental variables

441 (temperature, depth and nitrate:phosphate vertical flux) with a least squares multiple linear
442 regression model and the resulting equations used to estimate stoichiometric ratios across the
443 broader range of stations/depths (**Supplementary Table 5**). For both models the estimates of
444 cellular stoichiometric ratios were then scaled to the relative abundance of *Prochlorococcus*,
445 *Synechococcus*, and eukaryotes.

446 *Statistical Analyses*. All statistical analyses were done in SigmaStat Version 3.5 (Systat
447 Software, San Jose, CA).

448

449 **Acknowledgements:** We thank the Captains and crews of the various vessels that supported
450 these sea-going efforts. We thank Agathe Talarmin for sorting samples collected from the
451 SPOTS time-series and the Newport Pier. We thank Damian Grundle for inviting MWL on the
452 Sonne 243 cruise to collect samples in the Peru upwelling system. We acknowledge the National
453 Science Foundation for supporting our research (OCE-1046297, OCE-1559002 and OCE-
454 1848576 to ACM and OCE-1045966, OCE-1756054 and OCE-1756271 to MWL).

455

456 **Author Contributions:** MWL and ACM conceived the original idea. MWL wrote the
457 manuscript and prepared the figures with feedback and reviews from other authors. SEB, CM,
458 KXT, DAL and MAA all contributed to the at-sea collection and/or laboratory analysis of
459 samples presented in this manuscript.

460

461 **Competing interests:** All author(s) declare no competing interests.

462 **Data availability:** Data can be found under the corresponding authors name at the Biological-
463 Chemical Oceanography Data Management Office, Project title "Biological Control on the
464 Ocean C:N:P ratio" (<http://bco-dmo.org/project/2178>). Phytoplankton cell quota data from flow
465 cytometrically sorted natural populations has the following citation information: "Direct measure
466 of phytoplankton cell quotas from field populations sampled from multiple cruises cruises
467 between 2010 and 2016", 2021-06-03, DOI:10.26008/1912/bco-dmo.849153.1. Bulk data used
468 in the stoichiometric model portion of the manuscript can be found here: Lomas, M. W.,
469 Martiny, A. (2020) Depth profile data from R/V New Horizons NH1418 in the tropical Pacific
470 from Sept-Oct. 2014. Biological and Chemical Oceanography Data Management Office (BCO-
471 DMO). (Version 1) Version Date 2020-11-19, doi:10.26008/1912/bco-dmo.829895.1, and
472 Lomas, M. W., Martiny, A. (2020) Depth profile data from R/V Atlantic Explorer AE1319 in the
473 NW Atlantic from Aug-Sept. 2013. Biological and Chemical Oceanography Data Management
474 Office (BCO-DMO). (Version 1) Version Date 2020-11-18, doi:10.26008/1912/bco-
475 dmo.829797.1.

476

477 **References:**

478 1 Kwiatkowski, L., Aumont, O., Bopp, L. & Caias, P. The impact of variable phytoplankton
479 stoichiometry on projections of primary production, food quality and carbon uptake in the
480 global ocean. *Glob. Biogeochem. Cycle* **32**, 516-528 (2018).

481 2 Moreno, A. R. & Martiny, A. C. Ecological stoichiometry of ocean plankton. *Annual
482 Review of Marine Science* **10**, 43-69 (2018).

483 3 Redfield, A. in *James Johnstone Memorial Volume* 176-192 (Liverpool University
484 Press, 1934).

485 4 Redfield, A. The biological control of chemical factors in the environment. *American
486 Scientist* **46**, 205-221 (1958).

487 5 Martiny, A. C. *et al.* Strong latitudinal patterns in the elemental ratios of marine plankton
488 and organic matter. *Nature Geoscience* **6**, 279-283 (2013).

489 6 Sharoni, S. & Halevy, I. Nutrient ratios in marine particulate organic matter are predicted
490 by the population structure of well-adapted phytoplankton. *Science Advances* **6**,
491 eaaw9371 (2020).

492 7 Arrigo, K. *et al.* Phytoplankton community structure and the drawdown of nutrients and
493 CO₂ in the Southern Ocean. *Science* **283**, 35-367 (1999).

494 8 Weber, T. & Deutsch, C. Ocean nutrient ratios governed by plankton biogeography.
495 *Nature* **467**, 550-554 (2010).

496 9 Bertilsson, S., Berglund, O., Karl, D. M. & Chisholm, S. W. Elemental composition of
497 marine *Prochlorococcus* and *Synechococcus*: implications for the ecological
498 stoichiometry of the sea. *Limnol. Oceanogr.* **48**, 1721-1731 (2003).

499 10 Leonardos, N. & Geider, R. J. Responses of elemental and biochemical composition of
500 *Chaetoceros muelleri* to growth under varying light, nitrate:phosphate supply ratios and
501 their influence on the critical N:P. *Limnol. Oceanogr.* **49**, 2105-2114 (2004).

502 11 Rhee, G. Effect of N:P atomic ratios and nitrate limitation on algal growth, cell
503 composition, and nitrate uptake. *Limnol. Oceanogr.* **23**, 10-25 (1978).

504 12 Galbraith, E. & Martiny, A. C. A simple nutrient-dependence mechanism for predicting
505 the stoichiometry of marine ecosystems. *Proc. Acad. Nat. Sci. Phila.* **112**, 8199-8204
506 (2015).

507 13 Longhurst, A. R. *Ecological Geography of the Sea*. (Academic, 1998).

508 14 Frigstad, H. *et al.* Seasonal variation in marine C:N:P stoichiometry: can the composition
509 of seston explain stable Redfield ratios? *Biogeosciences* **8**, 2917-2933 (2011).

510 15 Tanioka, T., Fichot, C. & Matsumoto, K. Toward determining the spatio-temporal
511 variability of upper-ocean ecosystem stoichiometry from satellite remote sensing.
512 *Frontiers in Marine Science* **7**, 604893. doi: 604810.603389/fmars.602020.604893
513 (2020).

514 16 Talmy, D., Martiny, A., Hill, C., Hickman, A. & Follows, M. Microzooplankton
515 regulation of surface ocean POC:PON ratios. *Glob. Biogeochem. Cycle* **30**, 311-332
516 (2016).

517 17 Minor, E. C., Eglinton, T. I., Olson, R. & Boon, J. J. The compositional heterogeneity of
518 particulate organic matter from the surface ocean: an investigation using flow cytometry
519 and DT-MS. *Organic Geochemistry* **29**, 1561-+ (1998).

520 18 Baer, S., Lomas, M., Terpis, K., Mouginot, C. & Martiny, A. C. Stoichiometry of
521 *Prochlorococcus*, *Synechococcus*, and small eukaryotic populations in the western North
522 Atlantic Ocean. *Environ. Microbiol.* **19**, 1568-1583 (2017).

523 19 Garcia, C. *et al.* Nutrient supply controls particulate elemental concentrations and ratios
524 in the low latitude eastern Indian Ocean. *Nature Communications* **9**, 4868 (2018).

525 20 Casey, J., Aucan, J., Goldberg, S. & Lomas, M. Changes in partitioning of carbon
526 amongst photosynthetic pico- and nano-plankton groups in the Sargasso Sea in response
527 to changes in the North Atlantic Oscillation. *Deep Sea Research II* **93**, 58-70 (2013).

528 21 Martiny, A. C., Vrugt, J. A., Primeau, F. & Lomas, M. Regional variation in the
529 particulate organic carbon to nitrogen ratio in the surface ocean. *Glob. Biogeochem.*
530 *Cycle* **27**, 23-731 (2013).

531 22 Campbell, L., Nolla, H. A. & Vaulot, D. The importance of *Prochlorococcus* to
532 community structure in the central North Pacific Ocean. *Limnol. Oceanogr.* **39**, 955-961
533 (1994).

534 23 Landry, M. R. & Kirchman, D. L. Microbial community structure and variability in the
535 tropical Pacific. *Deep-Sea Res. Part II-Top. Stud. Oceanogr.* **49**, 2669-2693 (2002).

536 24 Heldal, M., Scanlan, D. J., Norland, S., Thingstad, F. & Mann, N. H. Elemental
537 composition of single cells of various strains of marine *Prochlorococcus* and
538 *Synechococcus* using X-ray microanalysis. *Limnol. Oceanogr.* **48**, 1732-1743 (2003).

539 25 Fuhrman, J. A., Sleeter, T. D., Carlson, C. A. & Proctor, L. M. Dominance of Bacterial
540 Biomass in the Sargasso Sea and Its Ecological Implications. *Mar. Ecol.-Prog. Ser.* **57**,
541 207-217 (1989).

542 26 Ho, T. *et al.* The elemental composition of some marine phytoplankton. *J. Phycol.* **39**,
543 1145-1159 (2003).

544 27 Whitney, L. P. & Lomas, M. W. Growth on ATP elicits a P-stress response in the
545 picoeukaryote *Micromonas pusilla*. *PLoS One* **11**, e0155158 (2016).

546 28 Whitney, L. P. & Lomas, M. W. Phosphonate utilization by eukaryotic phytoplankton.
547 *Limnology and Oceanography Letters* **4**, 18-24 (2019).

548 29 Hartmann, M. *et al.* Efficient CO₂ fixation by surface *Prochlorococcus* in the Atlantic
549 Ocean. *The ISME Journal* **8**, 2280-2289 (2014).

550 30 Cailliau, C., Claustre, H., Vidussi, F., Marie, D. & Vaulot, D. Carbon biomass, and gross
551 growth rates as estimated from C-14 pigment labelling, during photoacclimation in
552 *Prochlorococcus* CCMP 1378. *Mar. Ecol.-Prog. Ser.* **145**, 209-221 (1996).

553 31 Moore, L. R. & Chisholm, S. W. Photophysiology of the marine cyanobacterium
554 *Prochlorococcus*: Ecotypic differences among cultured isolates. *Limnol. Oceanogr.* **44**,
555 628-638 (1999).

556 32 Moore, L. R., Goericke, R. & Chisholm, S. W. Comparative Physiology of
557 *Synechococcus* and *Prochlorococcus* - Influence of Light and Temperature on Growth,
558 Pigments, Fluorescence and Absorptive Properties. *Mar. Ecol.-Prog. Ser.* **116**, 259-275
559 (1995).

560 33 Kana, T. M., Feiwel, N. L. & Flynn, L. C. Nitrogen starvation in marine *Synechococcus*
561 strains: clonal differences in phycobiliprotein breakdown and energy coupling. *Marine*
562 *Ecology* **88**, 75-82 (1992).

563 34 Green, B. R. What happened to the phycobilisome? *Biomolecules* **9**,
564 <https://doi.org/10.3390/biom9110748> (2019).

565 35 Stadnichuk, I. N. & Tropin, I. V. Antenna replacement in the evolutionary origin of
566 chloroplasts. *Microbiology* **83**, 299-314 (2014).

567 36 Boyd, P. W. & others, a. Marine phytoplankton temperature versus growth responses
568 from polar to tropical waters, outcome of a scientific community-wide study. *PLoS One*
569 **8**, e63091 (2013).

570 37 Raven, J. A. & Geider, R. J. Temperature and algal growth. *New Phytologist* **110**, 441-
571 461 (1988).

572 38 Fu, F. X., Warner, M. E., Zhang, Y., Feng, Y. & Hutchins, D. A. Effects of increased
573 temperature and CO₂ on photosynthesis, growth, and elemental ratios in marine
574 *Synechococcus* and *Prochlorococcus* (Cyanobacteria). *J. Phycol.* **43**, 485-496 (2007).

575 39 Martiny, A. C., Ma, L. Y., Mouginot, C., Chandler, J. W. & Zinser, E. R. Interactions
576 between thermal acclimation, growth rate, and phylogeny influence *Prochlorococcus*
577 elemental stoichiometry. *PLoS One* **11**, doi.org/10.1371/journal.pone.0168291 (2016).

578 40 Szul, M. J., Dearth, S. P., Campagna, S. R. & Zinser, E. R. Carbon fate and flux in
579 *Prochlorococcus* under nitrogen limitation. *mSystems* **4**, e00254-00218 (2019).

580 41 Van Mooy, B. A. S. *et al.* Phytoplankton in the ocean use non-phosphorus lipids in
581 response to phosphorus scarcity. *Nature*, doi:10.1038/nature07659 (2009).

582 42 Eppley, R. W. Temperature and phytoplankton growth in the sea. *Fishery Bulletin* **70**,
583 1063-1085 (1972).

584 43 Garcia, N. *et al.* High variability in cellular stoichiometry of carbon, nitrogen, and
585 phosphorus within classes of marine eukaryotic phytoplankton under sufficient nutrient
586 conditions. *Frontiers in Microbiology* **9** (2018).

587 44 Yvon-Durocher, G., Dossena, M., Trimmer, M., Woodward, G. & Allen, A. P.
588 Temperature and the biogeography of algal stoichiometry. *Global Ecology and*
589 *Biogeography* **24**, 562-570 (2015).

590 45 Toseland, S. *et al.* The impact of temperature on marine phytoplankton resource
591 allocation and metabolism. *Nature Climate Change* **3**, 979-984 (2013).

592 46 Geider, R. J. & LaRoche, J. Redfield revisited: variability of C:N:P in marine microalgae
593 and its biochemical basis. *Eur. J. Phycol.* **37**, 1-17 (2002).

594 47 Baer, S. E. *et al.* Carbon and nitrogen productivity during spring in the oligotrophic
595 Indian Ocean along the GO-SHIP IO9N transect. *Deep Sea Research II*, 81-91 (2019).

596 48 Cullen, J. & Eppley, R. W. Chlorophyll maximum layers of the South California Bight
597 and possible mechanisms of their formation and maintenance. *Oceanology Acta* **4**, 23-32
598 (1981).

599 49 Rhee, G. Y. & Gotham, I. J. The effect of environmental factors on phytoplankton
600 growth: Temperature and the interactions of temperature with nutrient limitation. *Limnol.*
601 *Oceanogr.* **26**, 635-648 (1981).

602 50 Saito, M. A., Goepfert, T. J. & Ritt, J. T. Some thoughts on the concept of colimitation:
603 Three definitions and the importance of bioavailability. *Limnol. Oceanogr.* **53**, 276-290
604 (2008).

605 51 Edwards, K. F. Mixotrophy in nanoflagellates across environmental gradients in the
606 ocean. *Proc. Acad. Nat. Sci. Phila.* **116**, 6211-6220 (2019).

607 52 Zubkov, M. V. & Tarran, G. A. High bacterivory by the smallest phytoplankton in the
608 North Atlantic Ocean. *Nature* **455**, 224-226 (2008).

609 53 Bertilsson, S., Berglund, O., Pullin, M. & Chisholm, S. W. Release of dissolved organic
610 matter by *Prochlorococcus*. *Vie Et Milieu-Life and Environment* **55**, 225-231 (2005).

611 54 Ammerman, J. W., Hood, R. R., Case, D. & Cotner, J. B. Phosphorus deficiency in the
612 Atlantic: an emerging paradigm in oceanography. *EOS* **84**, 165-170 (2003).

613 55 Lomas, M. W. *et al.* Sargasso Sea phosphorus biogeochemistry: an important role for
614 dissolved organic phosphorus (DOP). *Biogeosciences* **7**, 695-710 (2010).

615 56 Wu, J., Sunda, W., Boyle, E. & Karl, D. Phosphate depletion in the western North
616 Atlantic Ocean. *Science* **289**, 759-762 (2000).

617 57 van Mooy, B. A. S. & Devol, A. H. Assessing nutrient limitation of *Prochlorococcus* in
618 the North Pacific subtropical gyre by using an RNA capture method. *Limnol. Oceanogr.*
619 **53**, 78-88 (2008).

620 58 Garcia, N., Bonachela, J. A. & Martiny, A. C. Interactions between growth-dependent
621 changes in cell size, nutrient supply and cellular elemental stoichiometry of marine
622 *Synechococcus*. *ISME Journal* **10**, 2715-2724 (2016).

623 59 Kashtan, N. *et al.* Single cell genomics reveals hundreds of coexisting subpopulations in
624 wild *Prochlorococcus*. *Science* **344**, 416-420 (2014).

625 60 Pitt, F. *et al.* A sample-to-sequence protocol for genus targeted transcriptomic profiling:
626 application to marine *Synechococcus*. *Frontiers in Microbiology* **7**, doi:
627 10.3389/fmicb.2016.01592 (2016).

628 61 Lomas, M. W. & Martiny, A. C. Direct measure of phytoplankton cell quotas from field
629 populations sampled from multiple cruises cruises between 2010 and 2016. Biological
630 and Chemical Oceanography Data Management Office (BCO-DMO). (Version 1)
631 Version Date 2021-06-02. . doi:10.26008/21912/bco-dmo.849153.849151 (2021).

632 62 Gordon, L., Jennings, J., Jr., Ross, A. & Krest, J. A suggested protocol for continuous
633 flow automated analysis of seawater nutrients (phosphate, nitrate, nitrite, and silicic acid)
634 in the WOCE Hydrographic Program and the Joint Global Ocean Fluxes Study., 55
635 (Oregon State University, 1993).

636 63 Hydes, D. J. *et al.* Determination of dissolved nutrients (N, P, Si) in seawater with high
637 precision and inter-comparability using gas-segmented continuous flow analyzers.
638 IOCCP Report No. 14., 87 (2010).

639 64 Knap, A. *et al.* BATS Methods Manual Version 4. (U.S. JGOFS Planning Office, Woods
640 Hole, 1997).

641 65 Karl, D. M. & Tien, G. MAGIC: A sensitive and precise method for measuring dissolved
642 phosphorus in aquatic environments. *Limnol. Oceanogr.* **37**, 105-116 (1992).

643 66 Rimmelin, P. & Moutin, T. Re-examination of the MAGIC method to determine low
644 orthophosphate concentration in seawater. *Anal. Chim. Acta* **548**, 174-182 (2005).

645

646

647 **Figure Captions:**

648 **Figure 1.** Map of stations from which samples were collected and cell-sorted to quantify cellular
649 macronutrient content. Circled abbreviations represent the regions: North Atlantic Subpolar
650 (NASP), North Atlantic Subtropical Gyre (NASG), Coastal California (CCAL), Eastern Tropical
651 North Pacific (ETNP), North Pacific Subtropical Gyre (NPSG), Equatorial Pacific (EqPac),
652 Eastern Indian Ocean (EIO) and the Peru upwelling region (Peru UW). Specific cruise details
653 can be found in **Supplementary Table 1**. Dashed lines denote the separation between stations in
654 neighboring regions. Map created in Ocean Data View (Schlitzer, R., Ocean Data View,
655 <http://odv.awi.de>, 2014).

656

657 **Figure 2.** Biogeographical distribution of phytoplankton carbon, nitrogen and phosphorus
658 contents. (a) *Prochlorococcus*, (b) *Synechococcus*, and (c) eukaryotes, and in each, the upper
659 figure is the cellular elemental quota of carbon (Q_C), middle figure is the cellular elemental quota
660 of nitrogen (Q_N) and lower figure is the cellular elemental quota of phosphorus (Q_P). Regions
661 denoted on the x-axis are as defined in Figure 1. For *Prochlorococcus*, there are no data for
662 NASP and Peru UW as populations were either not present, or in too low an abundance to
663 reasonably achieve a sample for analysis. The yellow shaded regions in each panel represent
664 previously published cell content ranges: C - Casey et al.²⁰; N - Bertilsson et al.⁹ for
665 *Prochlorococcus* and *Synechococcus*, and Ho et al.²⁶ for picoeukaryotes; P - Bertilsson et al.⁹ for
666 *Prochlorococcus* and *Synechococcus*, and Ho et al.²⁶ and Whitney and Lomas^{27,28} for
667 picoeukaryotes.

668

669 **Figure 3.** Elemental stoichiometric ratios for each phytoplankton population in each ocean
670 region. Box-Whisker plots of (a) C:N (mol:mol), (b) C:P (mol:mol), and (c) N:P (mol:mol)
671 ratios for (L to R within a region) *Prochlorococcus*, *Synechococcus* and eukaryotes in each of the
672 eight ocean regions as noted at the top of panel (a) and defined in Figure 1. The box defines the
673 25% and 75% quartiles, the line through the box is the mean, the error bars represent the 5% and
674 95% distribution limits, and black circles represent data points outside this range. Where there
675 are no box/whisker plots, there are no available data.

676

677 **Figure 4.** Relationship of cellular stoichiometric ratios to vertical nitrate:phosphate fluxes across
678 the nutricline. (a-c) *Prochlorococcus*; (d-f) *Synechococcus*; and (g-i) Eukaryote populations and
679 C:N (a, d, g), C:P (b, e, h), and N:P (c, f, i) ratios (mol:mol).

680

681 **Figure 5.** Measured and modeled euphotic zone particulate carbon-to-phosphorus stoichiometric
682 ratios. Euphotic zone averaged particulate organic carbon-to-phosphorus (C:P) stoichiometric
683 ratios along (a) a transect in the western North Atlantic Ocean and (b) a transect in the central
684 Tropical/Equatorial Pacific. The black line is the euphotic zone (0-100m) average ratio of bulk

685 POM measurements, and the grey shading is the 95% confidence interval around the euphotic
686 zone average ratio. The red line is the optimal-growth phytoplankton model estimate of
687 particulate C:P ratio, and the blue line is the acclimation model estimate of particulate C:P ratio.
688 For both models, the error bars at each station represent the 95% confidence interval range. The
689 western North Atlantic transect was comprised of two cruises, both in August/September, with
690 the northern half (31°N – 55°N) conducted in 2013 (Cruise AE1319), and the southern half (19°N
691 – 33°N) conducted 2014 (BVal 47). The central Tropical/Equatorial Pacific transect was a single
692 cruise (NH1418). Significant differences between models and observations at each station are
693 represented in the following manner: ‘a’ – observations are significantly different from the
694 predictions of the optimal-growth model; ‘b’ – predictions from the optimal-growth model are
695 significantly different from the predictions of the acclimation model; and ‘c’ – observations are
696 significantly different from the predictions of the acclimation model. Above each panel is a
697 stacked area plot of the relative contribution of cyanobacteria *Prochlorococcus* (green fill),
698 *Synechococcus* (orange fill) and eukaryotes (grey fill) to total measured autotrophic C along the
699 transect.

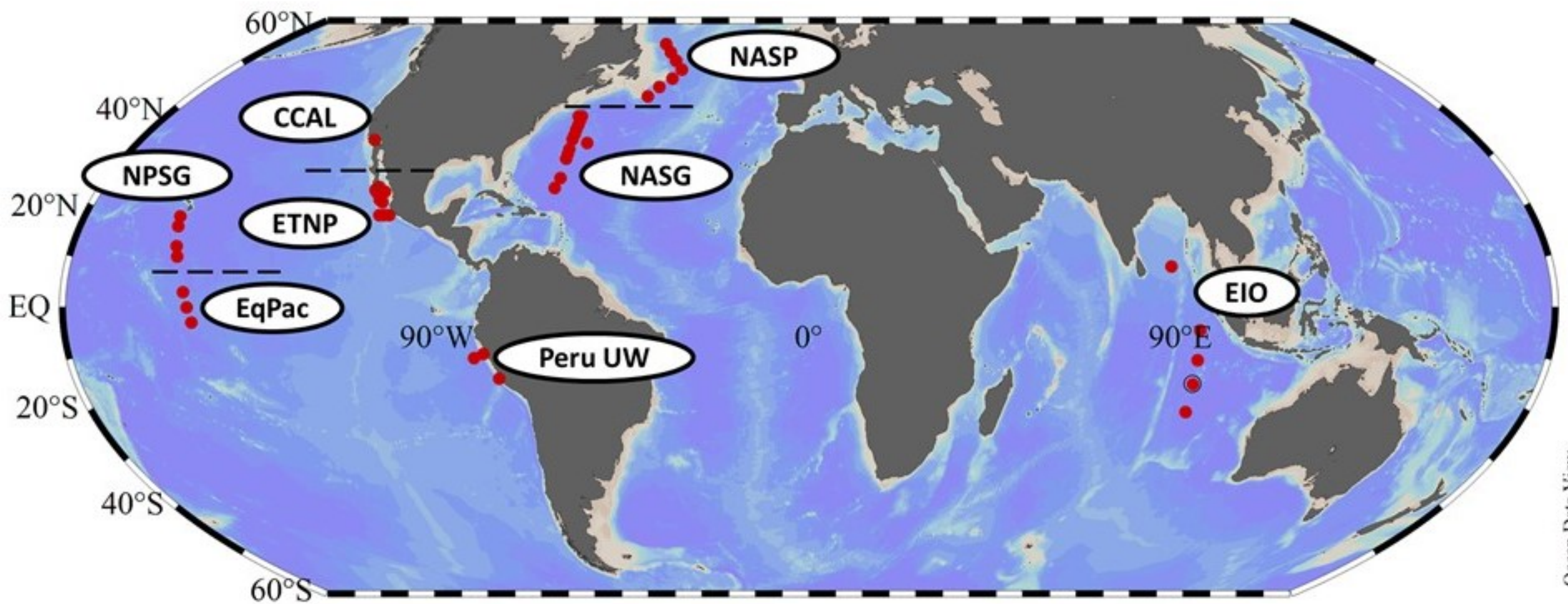
700

701 **Table 1.** Correlations between measured environmental variables and cellular contents and
 702 stoichiometric ratios for each taxonomic group. Correlations were tested using the Pearson
 703 Product Moment Correlation test for each taxa/element content pair and selected environmental
 704 variables. Strength of correlation (R), significance of correlation (P-value) and number of
 705 discrete data points in the correlation (N) are shown for each correlation. Significant (P-value
 706 <0.05) correlations are shown in bold font, marginally significant (P-value >0.05 <0.10)
 707 correlations are shown in italics.

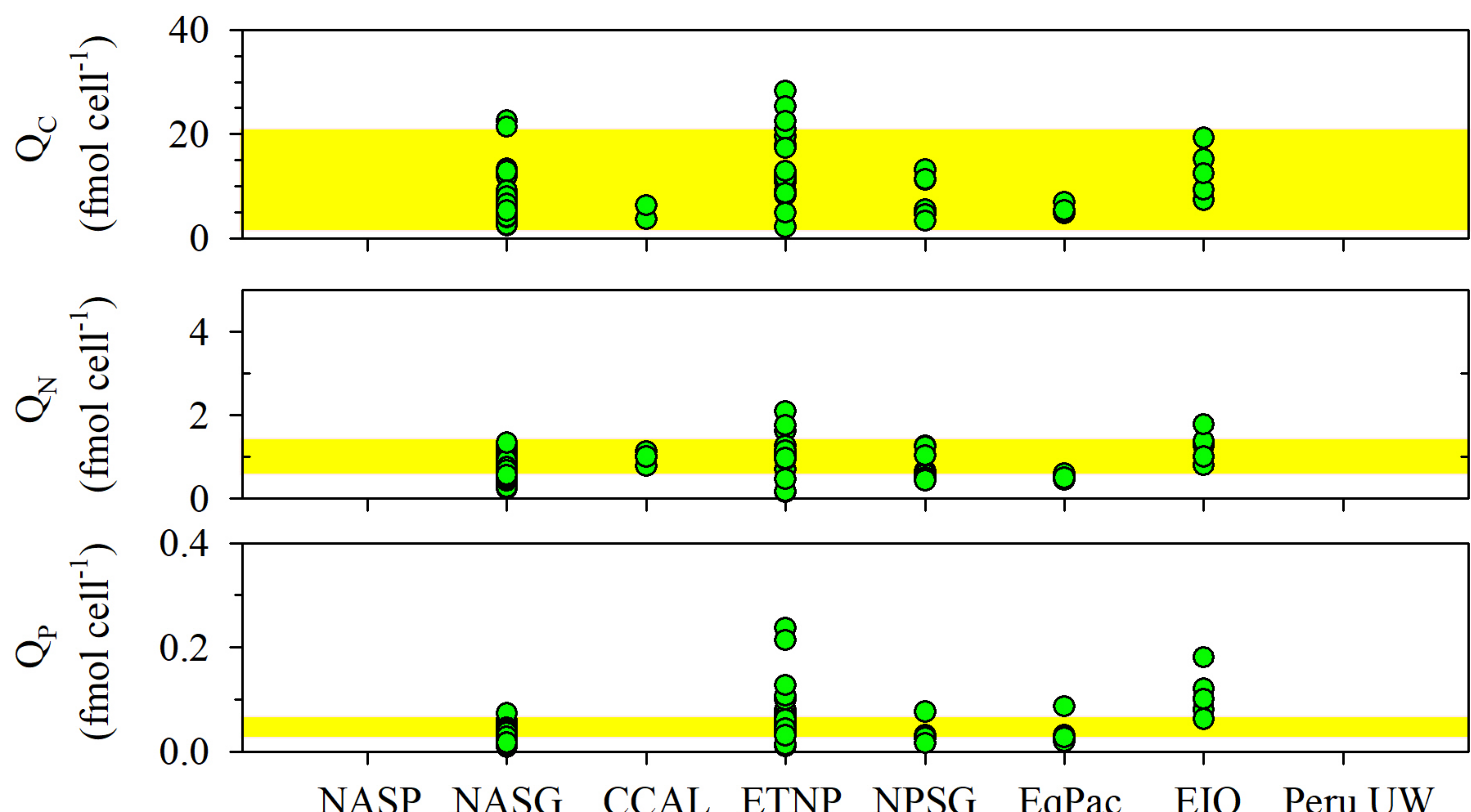
708

Taxa	Para- meter	Depth (irradiance proxy)			Temperature			NO ₃ :PO ₄ flux		
		R	P- value	N	R	P- value	N	R	P- value	N
<i>Prochlorococcus</i>	C	0.41	<0.01	84	-0.29	<0.01	74	-0.31	<0.01	70
	N	0.15	0.17	81	0.04	0.77	67	-0.27	0.03	67
	P	<i>0.21</i>	<i>0.08</i>	72	-0.13	0.28	66	-0.26	0.04	65
	C:N	0.29	<0.01	85	-0.46	0.01	73	-0.22	0.07	73
	C:P	0.10	0.44	62	-0.08	0.58	56	0.35	<0.01	55
	N:P	-0.18	0.17	59	0.25	0.08	53	0.69	<0.01	52
<i>Synechococcus</i>	C	0.04	0.72	70	-0.21	0.13	56	-0.32	0.02	56
	N	0.28	0.02	64	-0.20	0.16	50	-0.03	0.82	51
	P	0.11	0.41	60	-0.35	0.02	42	-0.38	0.02	41
	C:N	-0.09	0.49	60	-0.29	0.05	50	0.01	0.97	51
	C:P	-0.19	0.19	49	0.28	0.07	41	0.32	0.05	40
	N:P	-0.19	0.21	47	0.27	0.12	35	0.33	0.06	34
Eukaryotes	C	0.06	0.60	87	0.22	0.06	73	-0.14	0.22	76
	N	0.11	0.34	84	0.15	0.23	71	-0.11	0.34	71
	P	-0.01	0.95	74	0.21	0.12	59	0.10	0.46	58
	C:N	-0.05	0.67	75	0.01	0.91	70	0.31	<0.01	71
	C:P	-0.29	0.04	52	0.43	<0.01	49	0.37	<0.01	49
	N:P	0.13	0.36	51	0.28	0.07	45	0.35	0.02	45

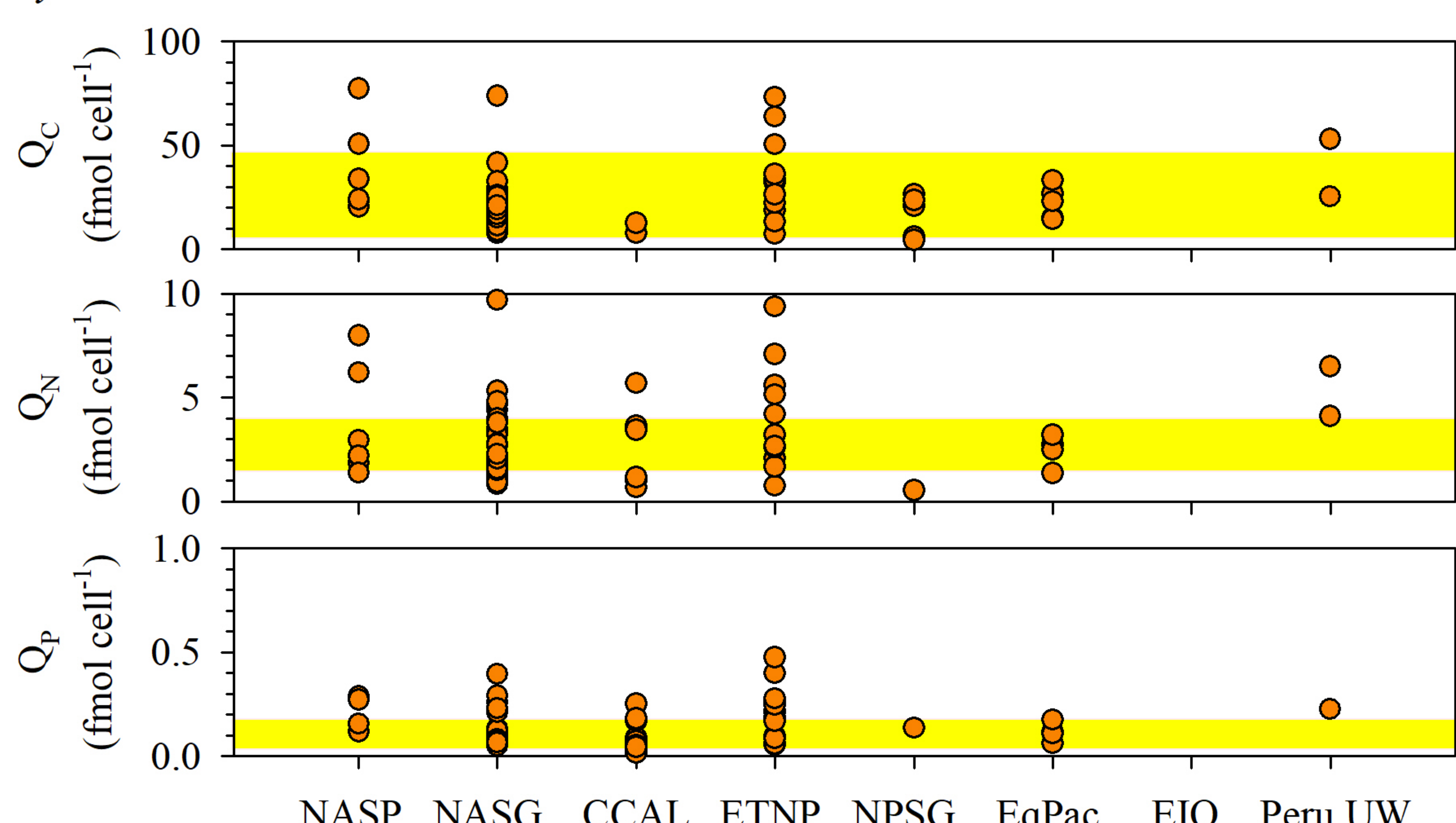
709



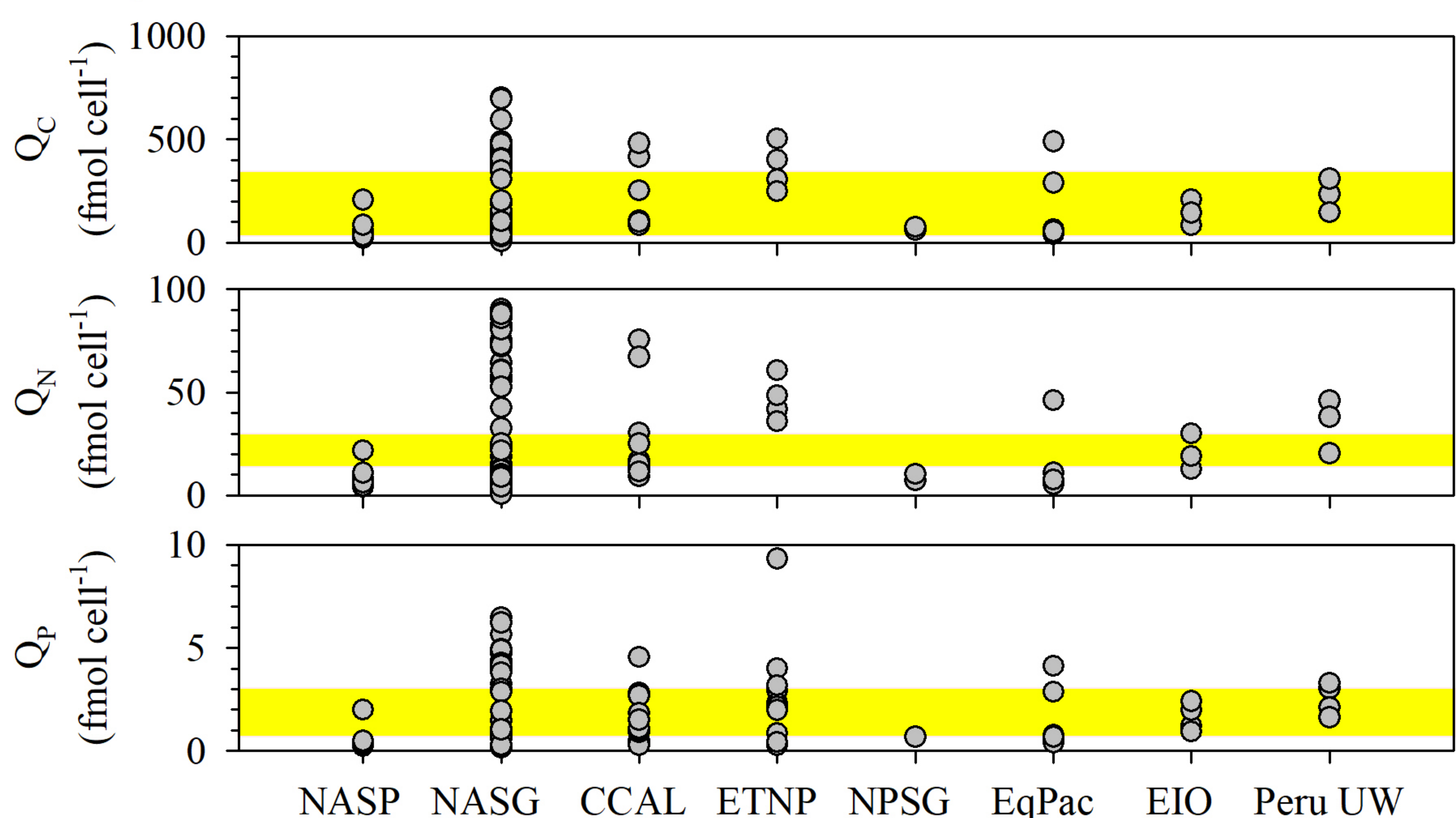
(a) *Prochlorococcus*

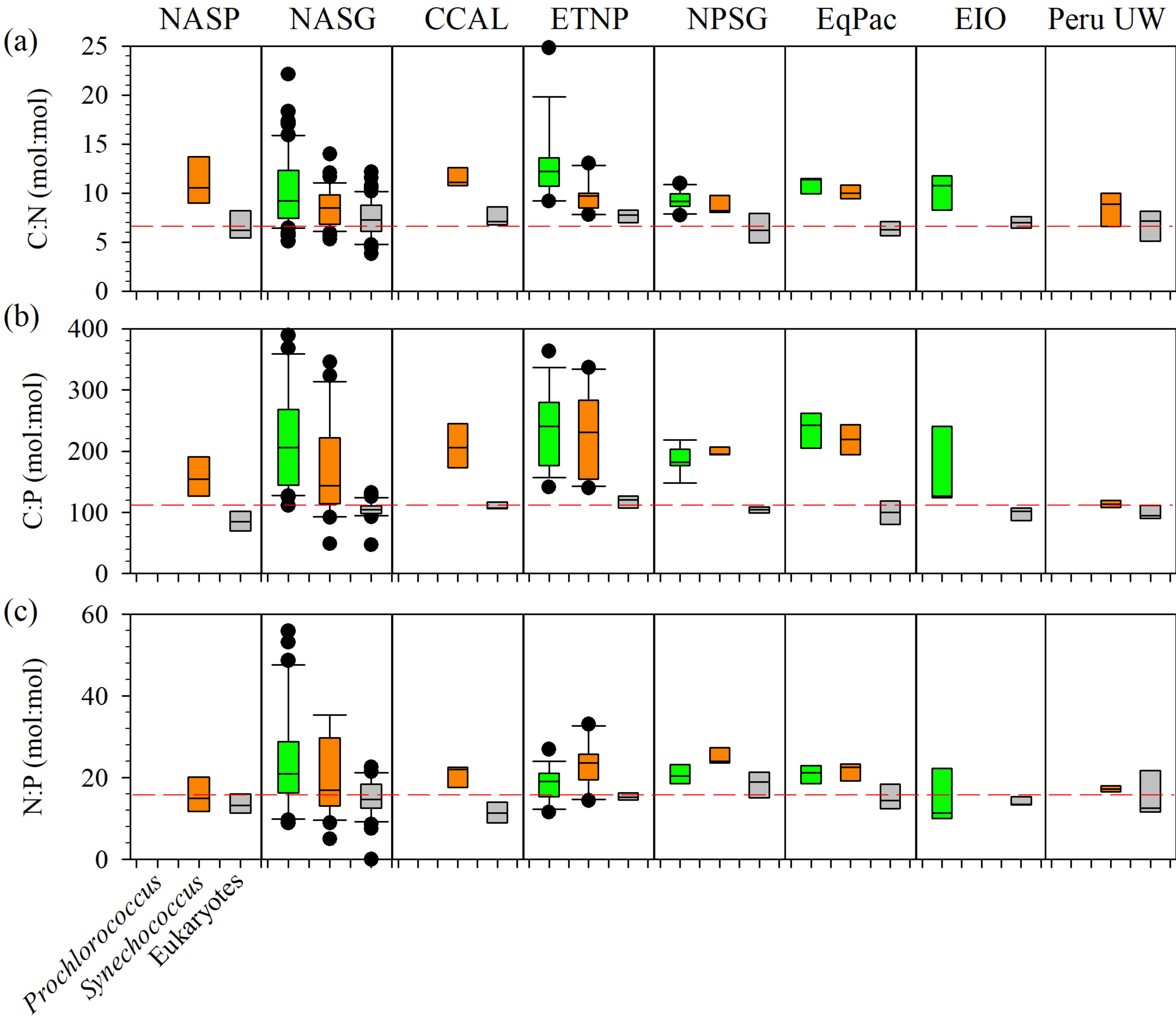


(b) *Synechococcus*

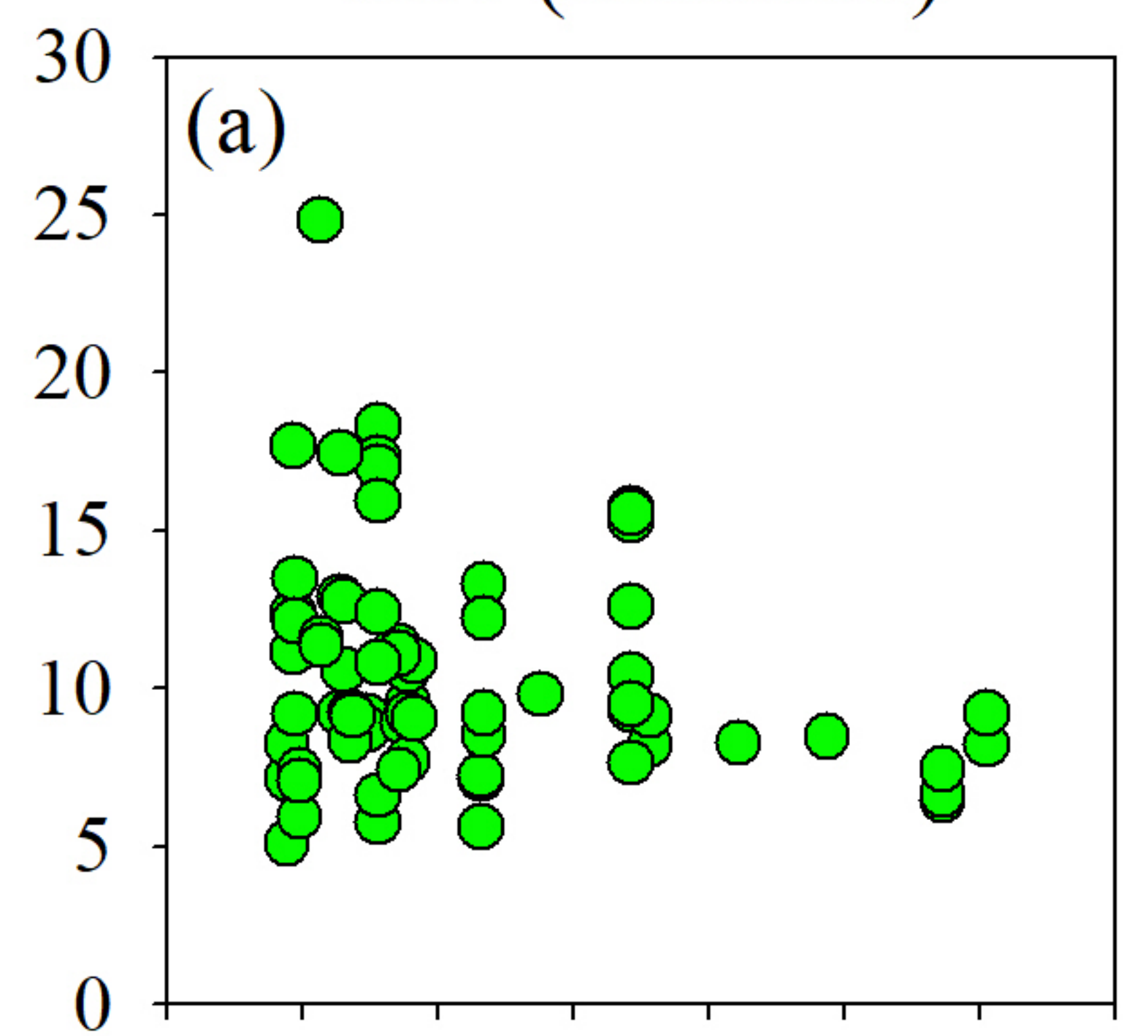


(c) Eukaryotes

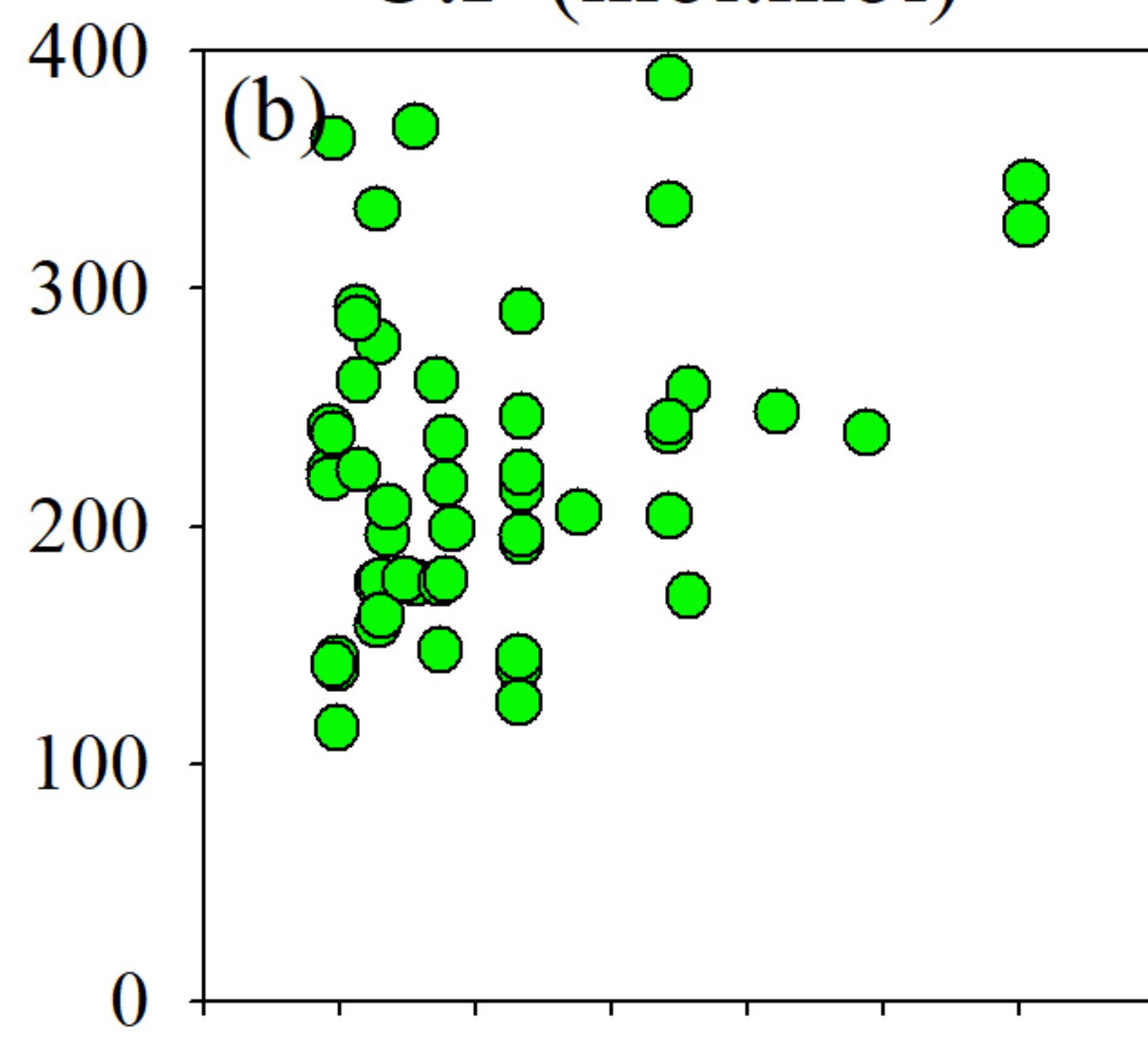




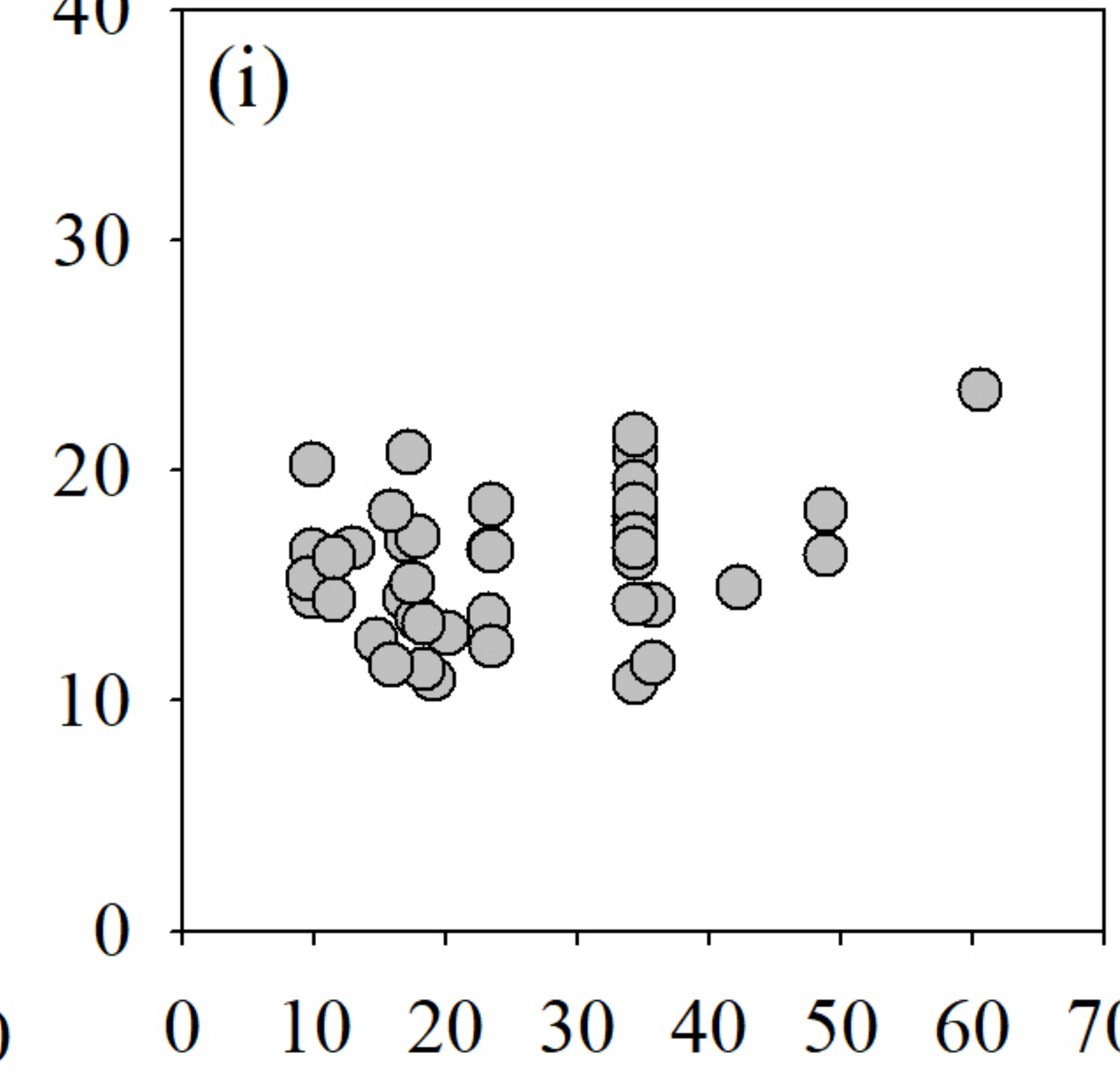
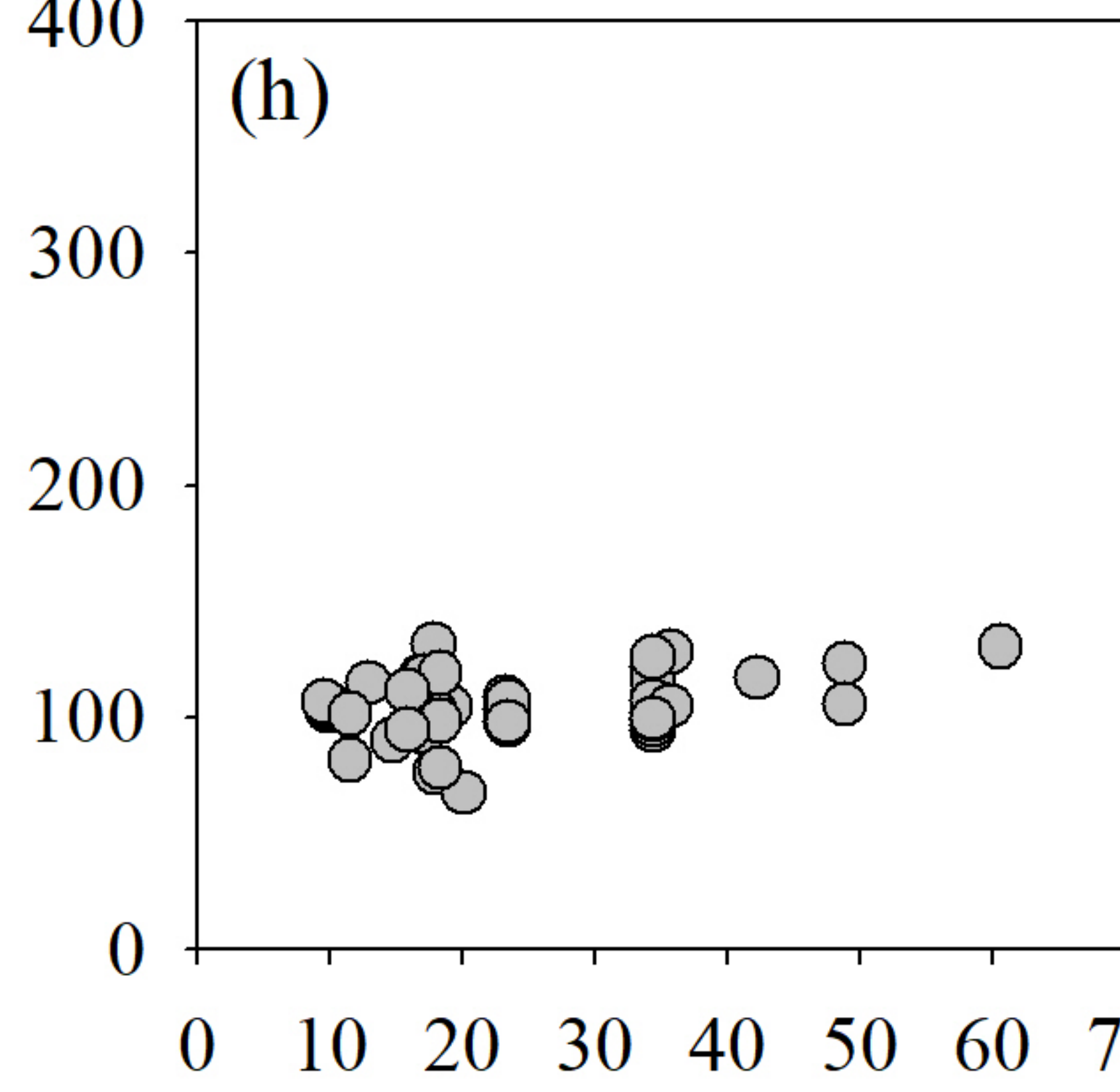
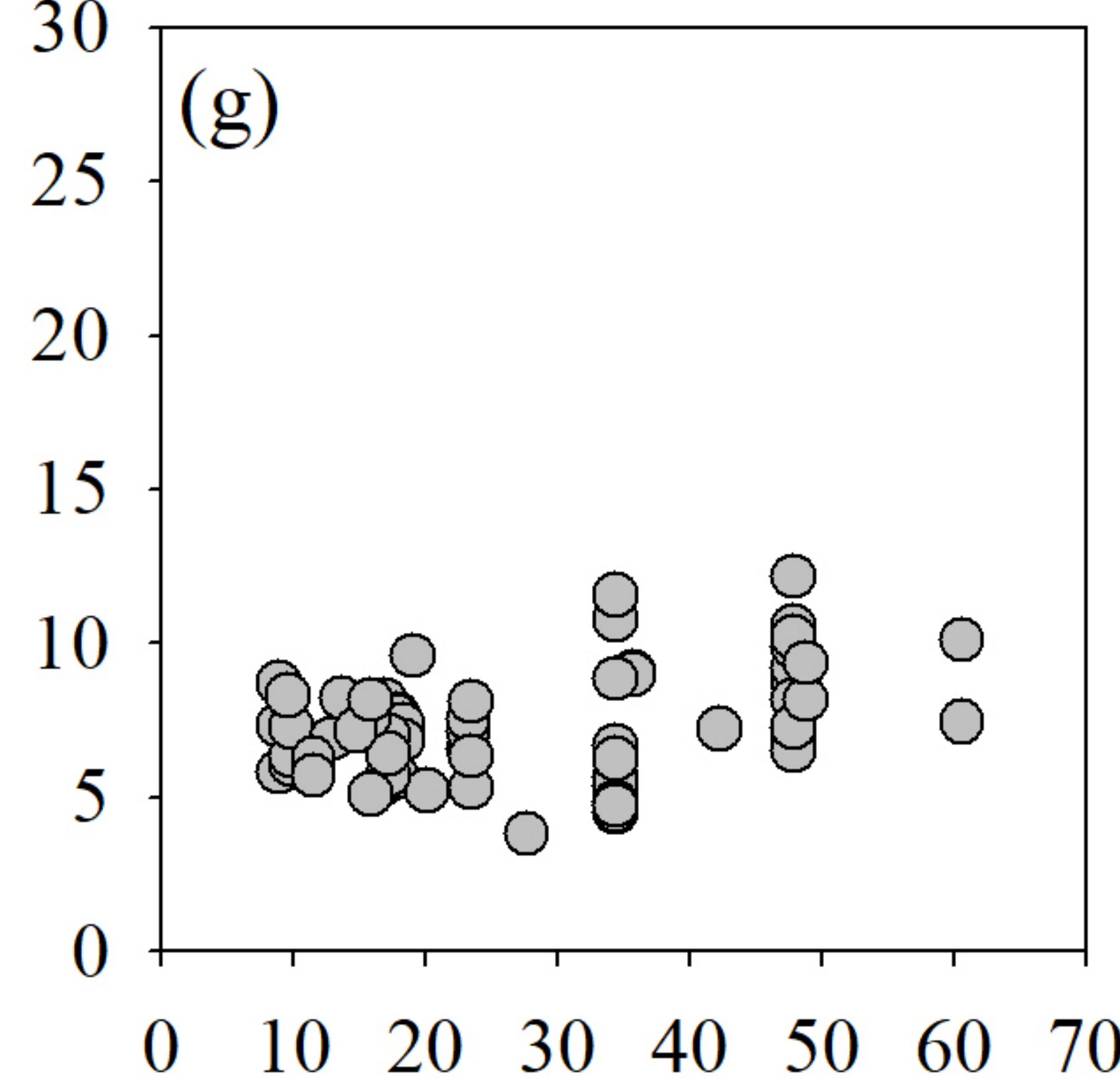
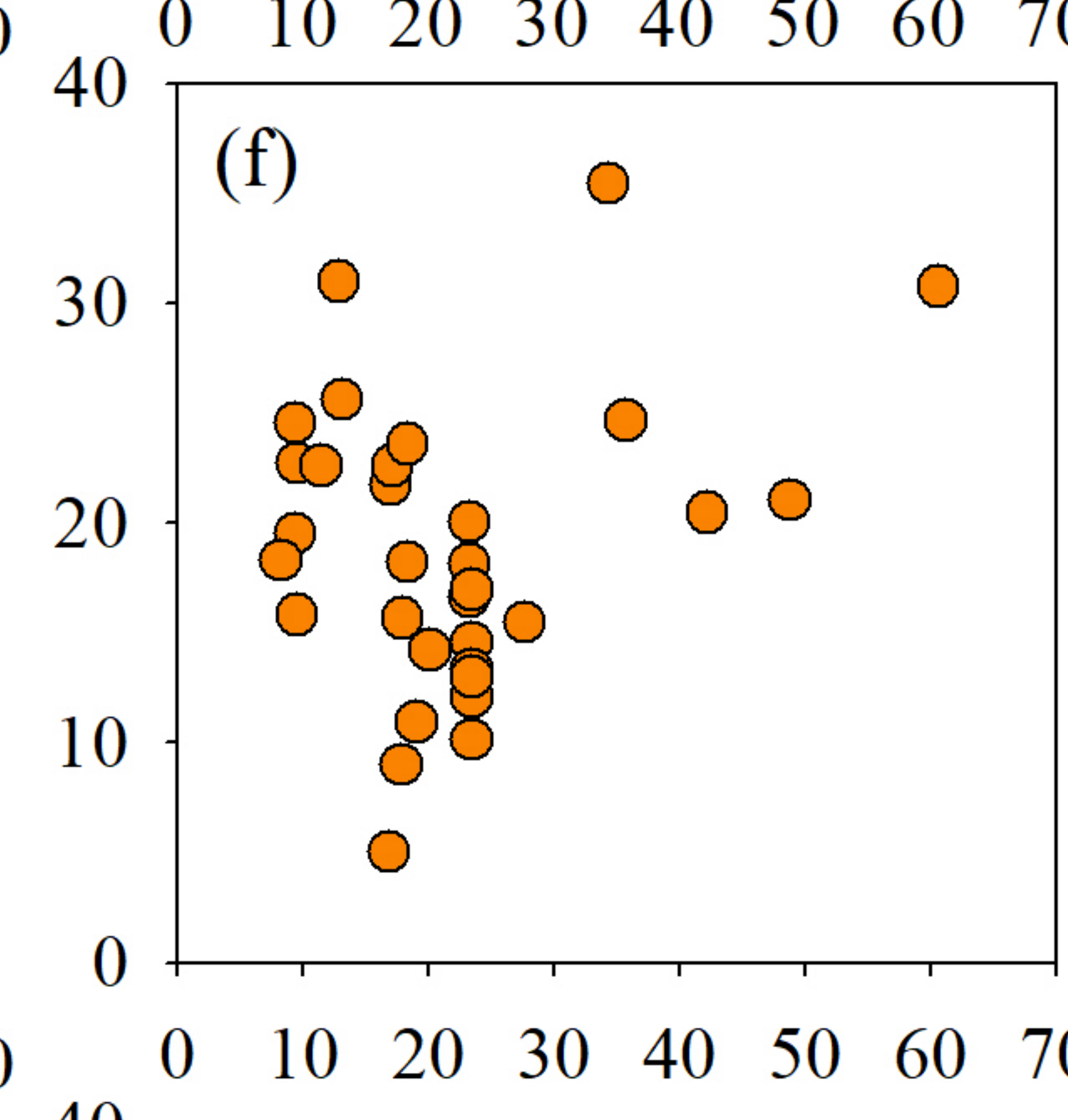
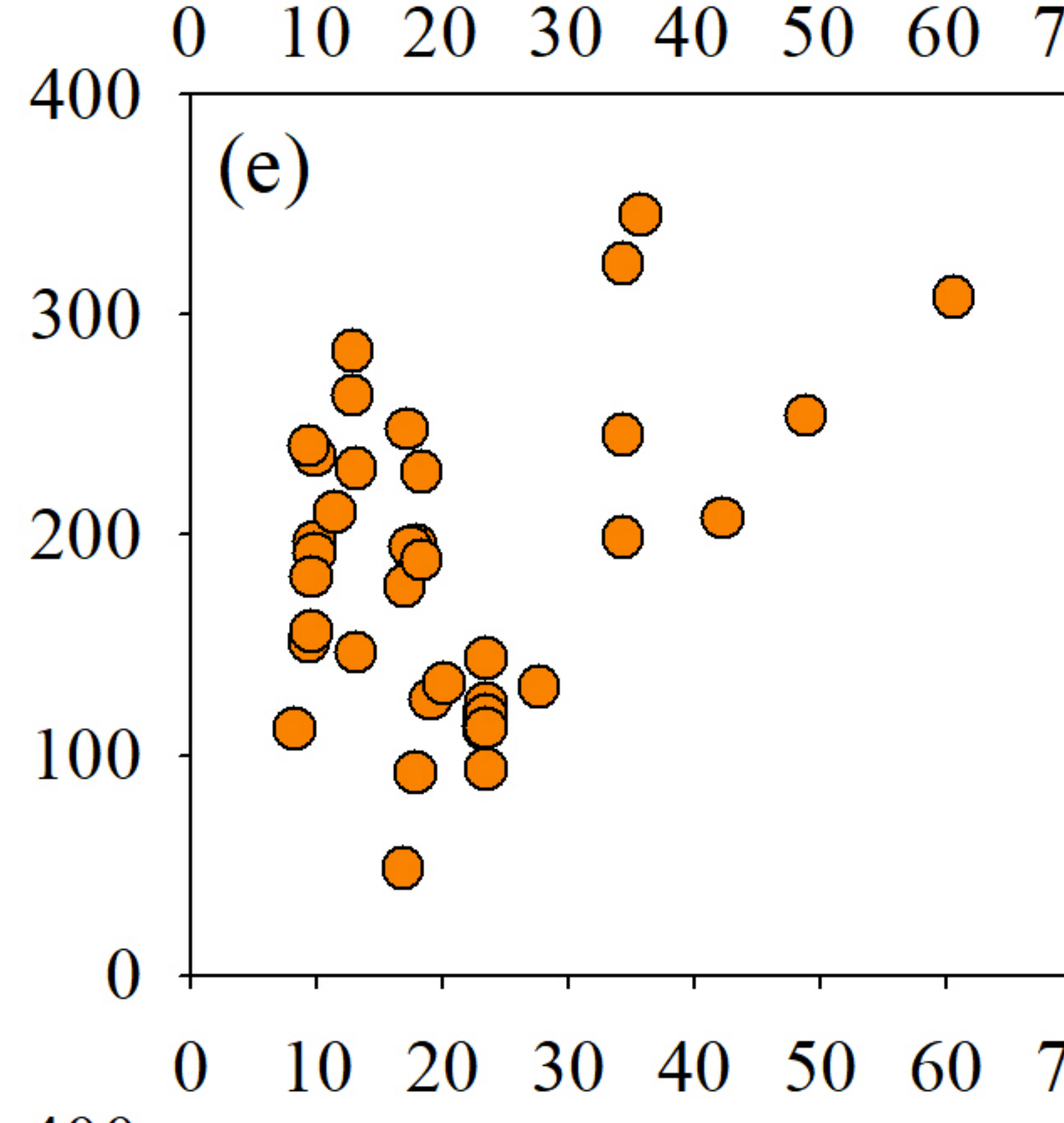
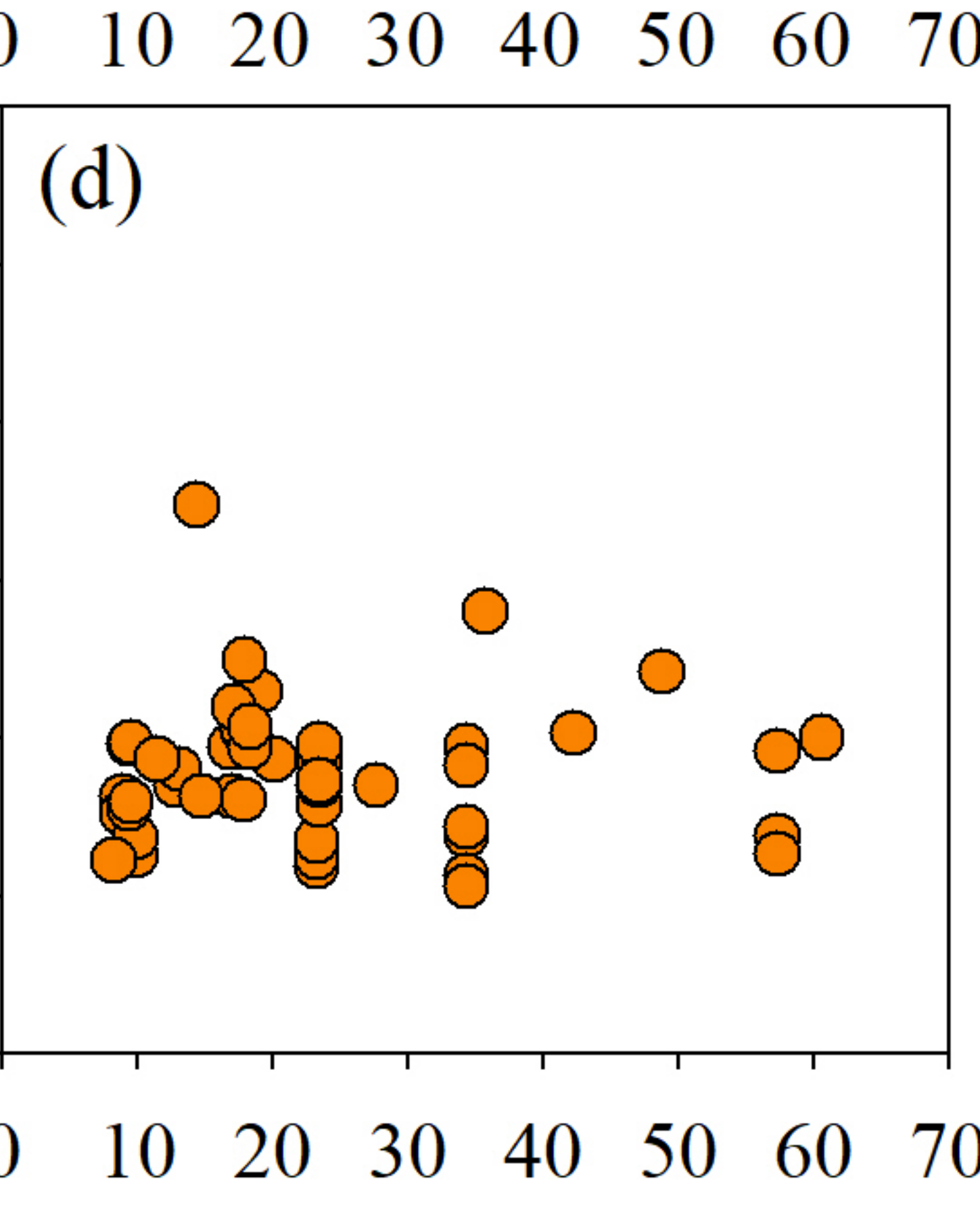
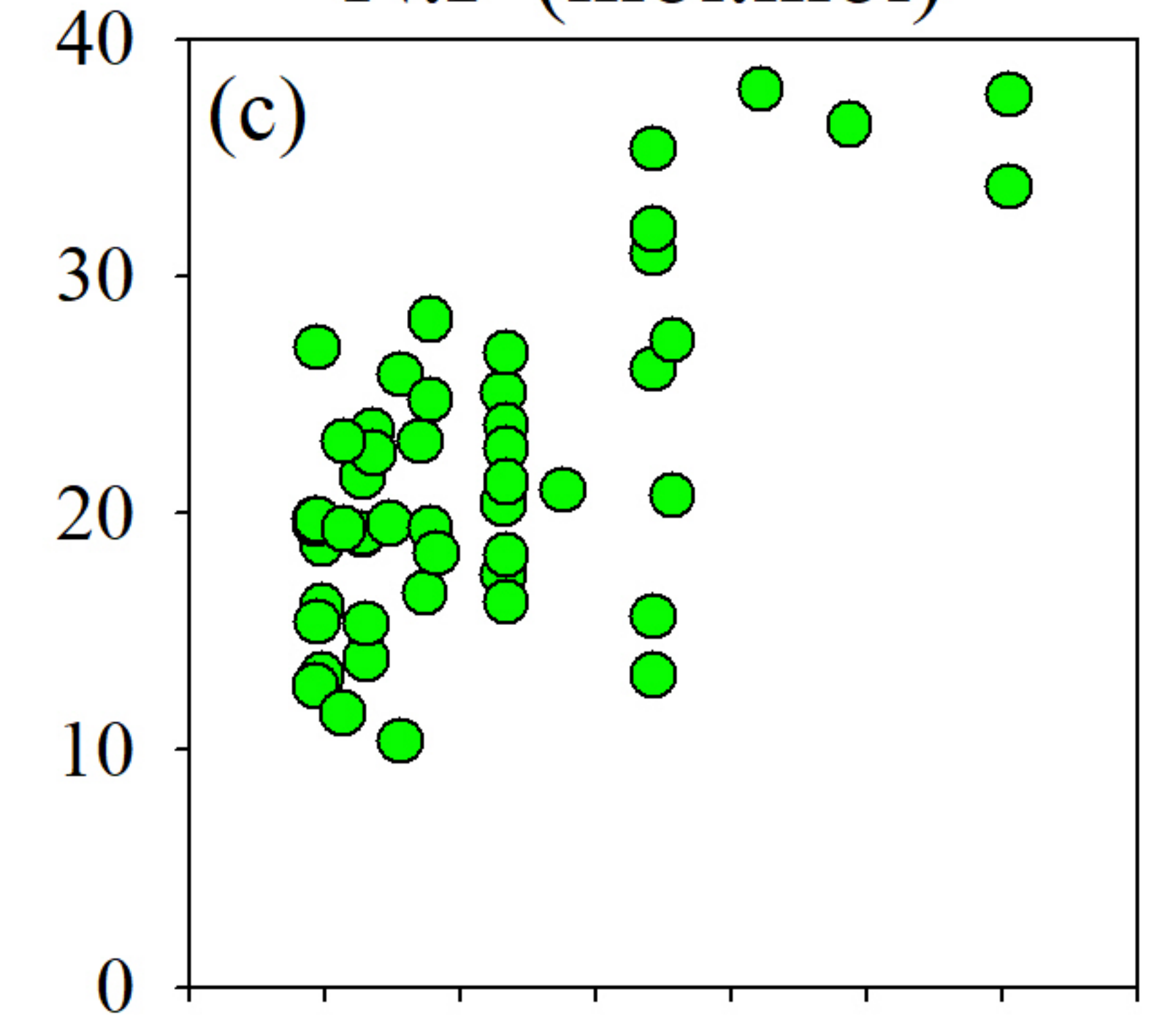
C:N (mol:mol)



C:P (mol:mol)

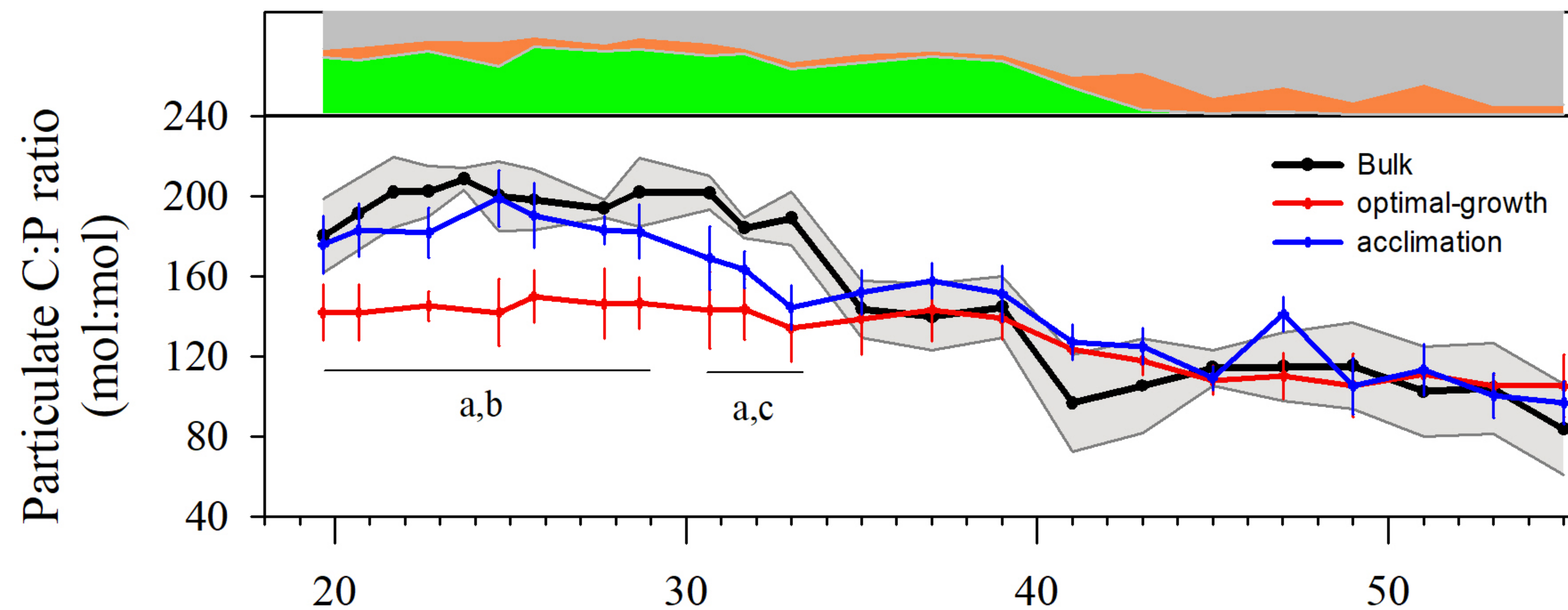


N:P (mol:mol)



nitrate:phosphate flux (mol:mol)

(a) Western Subpolar/Subtropical North Atlantic Transect



(b) Central Tropical/Equatorial Pacific Transect

